Small UAS Detect and Avoid Requirements Necessary for Limited Beyond Visual Line of Sight (BVLOS) Operations: Task 6 UND June 2021 Flight Test Report

March 11, 2022

NOTICE

LEGAL DISCLAIMER

Technical Report Documentation Page

1. Report No.	2. Government Accession No.	3. Recipient's Catalog No.
DOT/FAA/AR-xx/xx		
4. Title and Subtitle TITLE OF REPORT Small UAS Detect and Avoid Requirements Necessary for Limited Beyond Visual Line of Sight (BVLOS) Operations: Task 6 UND June 2021 Flight Test Report		5. Report Date March 11, 2022 6. Performing Organization Code ASSURE: University of North Dakota
7. Author(s) Mark Askelson and Amy Stephens		8. Performing Organization Report No.
9. Performing Organization Name and Address University of North Dakota Tech Accelerator Room 2050 4201 James Ray Dr Stop 8367 Grand Forks, ND 58202-8367		10. Work Unit No. (TRAIS) 11. Contract or Grant No. 15-C-UAS
12. Sponsoring Agency Name and Address U.S. Department of Transportation Federal Aviation Administration Washington, DC 20591		13. Type of Report and Period Covered Interim Report 14. Sponsoring Agency Code
15. Supplementary Notes		

16. Abstract

The demand for Beyond Visual Line Of Sight (BVLOS) operations using small Unmanned Aircraft Systems (sUASs) is high. A major impediment to realization of these operations is the Detect And Avoid (DAA) function. Two critical DAA challenges are definition of sUAS DAA system performance requirements and development of test methods for those performance requirements. The ASTM (American Society for Testing and Materials) WK62668 Detect and Avoid Performance Requirements Task Group has developed proposed performance requirements for sUAS DAA. The ASTM WK62669 DAA Test Methods Task Group is currently developing test methods for evaluating compliance of sUAS DAA systems with performance requirements. This effort is informing the ASTM WK62669 DAA Test Methods Task Group.

A flight test method that is part of a broader testing approach that also involves simulation, lab testing, etc., is described herein. This test method leverages a geometric approach to gathering data, in which potential encounter geometries are varied. Justification for the subset chosen herein, including how it relates to the broader set of encounters, is provided. Relative to previous efforts, descend-into encounters were added to the set off encounter scenarios.

Analysis methods were modified, relative to previous efforts, to include a coast period that occurs at the end of the maneuver period. This is needed owing to the Uncrewed Aircraft (UA) reaching the visual range limit associated with Part 107 operations prior to the time when aircraft separation is minimized.

No horizontal well clear violations occurred during this test campaign, resulting in a loss of well clear risk ratio for this subset of encounter scenarios of 0.0. Uncertainty windows for this subset of encounters ranged from 0.0-0.01 to 0.0-0.02. The exceptional performance of the UA that was used in these tests—especially its cruising speed, significantly enabled maintenance of horizontal well clear.

These results support the ASTM WK62669 DAA Test Methods Task Group through identification of metrics that characterize DAA system performance. Moreover, metrics that can be used for comparison with simulation results, which comprise an overall strategy for demonstrating compliance with performance requirements, are suggested. This includes a new metric for characterization of aircraft separation/risk.

17. Key Words	18. Distribution Statement
Test Plan Detect and Avoid Standards	This document is available to the U.S. public through the National Technical Information Service (NTIS), Springfield, Virginia 22161. This document is also available from the Federal Aviation Administration William J. Hughes Technical Center at actlibrary.tc.faa.gov.

19. Security Classif. (of this report)	20. Security Classif. (of this page)	21. No. of Pages	22. Price
Unclassified	Unclassified	75	

Form DOT F 1700.7 (8-72) Reproduction of completed page authorized

TABLE OF CONTENTS

TABLE OF FIGURES

TABLE OF TABLES

TABLE OF ACRONYMS

Acronym	Meaning
2D	Two-Dimensional
A&G	Alerting and Guidance
A1F	Alert Function
A2F	Avoid Function
ADS-B	Automatic Dependent Surveillance-Broadcast
AGL	Above Ground Level
ASTM	American Society for Testing and Materials
BVLOS	Beyond Visual Line Of Sight
CA	Crewed Aircraft
CDF	Cumulative Density Function
CE	Climb-into Encounter
CFl	Coasted Flag
CFR	Code of Federal Regulations
CPA	Closest Point of Approach
DAA	Detect And Avoid
DCAPS	Data Collection and Processing System
DE	Descend-into Encounter
DF	Detect Function
DTEM	Detect, Track, Evaluate, and Maneuver
DVR	Digital Video Recorder
EFP	Encounter Focal Point
EO	Electronic Observer
FAA	Federal Aviation Administration
FoV	Field of View
FTD	Flight Test Director
FTR	False Target Rating
GBDAA	Ground Based Detect And Avoid
GCS	Ground Control System
GPS	Global Positioning System
HE	Horizontal Encounter
HITL	Human In The Loop
LR	Well Clear Risk Ratio
LRE	Launch and Recovery Element
LTE	Long-Term Evolution
MC	Mission Commander
MSU	Mississippi State University
NMAC	Near Mid-Air Collison
NPUASTS	Northern Plains UAS Test Site
NTIS	National Technical Information Service
OEP	Objective Encounter Period
PDF	Probability Density Function
PI	Principal Investigator
PIC	Pilot in Command
RR	NMAC Risk Ratio
SBS	Surveillance and Broadcast Services
SBSS	Surveillance and Broadcast Services Subsystem
SPS	Standard Positioning Service
sUAS	Small Uncrewed Aircraft System
SWaP	Size, Weight, and Power
TPTRT	Time Prior To Reference Time

UA	Uncrewed Aircraft
UAS	Uncrewed Aircraft System
uCPA	Unmitigated Closest Point of Approach
UND	University of North Dakota
UPS	Uninterruptable Power Supply
UTC	Universal Time Coordinated
VAS	Value Added Service
VHF	Very High Frequency
VTOL	Vertical Take-Off and Landing
WAAS	Wide Area Augmentation System
WCV	Well Clear Violation

EXECUTIVE SUMMARY

The demand for Beyond Visual Line Of Sight (BVLOS) operations using small Uncrewed Aircraft Systems (sUASs) is high. A major impediment to realization of these operations is the Detect And Avoid (DAA) function. Several challenges exist for sUAS DAA. Of these, two critical challenges are definition of sUAS DAA system performance requirements and development of test methods for those performance requirements. The American Society for Testing and Materials (ASTM) WK62668 DAA Performance Requirements Task Group has developed proposed performance requirements for sUAS DAA. The ASTM WK62669 DAA Test Methods Task Group is currently developing test methods for evaluating compliance of sUAS DAA systems with performance requirements. This effort is informing the ASTM WK62669 DAA Test Methods Task Group. In addition, as part of the project "A18_ A11L.UAS.22 – Small UAS Detect and Avoid Requirements Necessary for Limited Beyond Visual Line of Sight (BVLOS) Operations: Separation Requirements and Testing" (A18), this report also describes development of a test plan for sUAS DAA systems and evaluation of that test plan. The fundamental questions are:

- How can flight tests be designed to provide the needed information for evaluation of compliance with DAA performance requirements? How much testing (how many encounters) and what types (are) needed?
- How can flight tests be designed to ensure safety during the testing process?
- What data elements are needed for evaluation of compliance with performance requirements?

This report builds upon the results of Askelson (2022) by expanding the types of encounters tested, analyzing impacts of changes to the number of encounters executed for chosen encounter scenarios, and further exploring metrics/encounter characteristics that enable evaluation of compliance with performance requirements.

This report describes a flight test method that is part of a broader testing approach that also involves simulation, lab testing, etc. This test method leverages a geometric approach to gathering data, in which potential encounter geometries are varied. In addition to horizontal encounters, descend-into encounters (intruder descends) were also executed. Pragmatic drivers, including time and cost, resulted in a subset of the total number of possible encounters being evaluated. This report describes how these encounters were executed and how safety margins are maintained. Based upon this work, further insight regarding how results from flight tests can be related to simulation-based results as part of an overall test method approach to the ASTM WK62669 DAA Test Methods Task Group is provided—including a new metric for characterization of aircraft separation/risk). This continues to be a major challenge faced by this group—how to validate simulations using flight test data.

The vertical aircraft safety offset was increased 50 ft relative to that used by Askelson (2022) to 400 ft. This helped ensure desired aircraft separation. The biggest enabler for ensuring maintenance of vertical well clear during testing, however, was Crewed Aircraft (CA) altitude monitoring in which CA altitudes were adjusted if they were deemed to be too low. These resulted in no vertical well clear violations occurring during the June 2021 test campaign. For descend-into encounters, CA descent was halted to preserve a 400 ft vertical safety offset between aircraft.

The pilots were successful at halting their descent as planned, as the minimum vertical offset for the 10 descend-into encounters was 403 ft.

In addition to metrics developed by Askelson (2022), an encounter descriptor/metric labelled coast period was added. This is needed because of flight of the Uncrewed Aircraft (UA) under Part 107 rules, without the use of daisy-chained observers, and the speed of the UA resulting in it reaching the visual range limit associated with Part 107 prior to the time when aircraft separation was minimized. When that limit was reached, the aircraft was directed to station-keep (fly circles around a defined location). To obtain results consistent with a BVLOS type of operation in which such station-keeping would not generally occur, the straight-line portion of the UA path associated with its maneuver was extrapolated forward/coasted.

Execution of more encounters for given scenarios did not consistently reduce the standard deviation of the aircraft separation metric analyzed herein. It did, however, reduce uncertainty in both the mean and standard deviations of that metric.

No horizontal well clear violations occurred during this test campaign, resulting in a loss of well clear risk ratio for this subset of encounter scenarios of 0.0. Uncertainty windows for this subset of encounters ranged from 0.0-0.01 to 0.0-0.02. The exceptional performance of the SuperVolo UA that was used in these tests—especially its cruising speed (up to ~66 kts), significantly enabled maintenance of horizontal well clear.

This report identifies topics deserving of further evaluation. These include addition of other variations in flight tests (e.g., curved trajectories) and definition of agreement/correspondence between simulations and flight tests. Some future research directions will likely arise as the ASTM WK62669 DAA Test Methods Task Group continues to integrate these findings into its standard.

1 INTRODUCTION

One of the fundamental tasks in this project, "A18_ A11L.UAS.22 – Small UAS Detect and Avoid Requirements Necessary for Limited Beyond Visual Line of Sight (BVLOS) Operations: Separation Requirements and Testing" (A18), is development of a test plan for small Uncrewed Aircraft System (sUAS) Detect And Avoid (DAA) systems and evaluation of that test plan. This report describes the tests conducted at the University of North Dakota (UND) by the UND and Northern Plains UAS Test Site (NPUASTS) during the week of 13-19 June 2021. This includes the test plan, test results, and lessons learned.

2 TEST PLAN

Below, UND provides an overview of the test plan. The reader is referred to the overarching A18 test plan "Small UAS Detect and Avoid Requirements Necessary for Limited Beyond Visual Line of Sight (BVLOS) Operations: Separation Requirements and Testing: (Overarching) Test Plan" for additional context.

2.1 Background

2.1.1 Standards Efforts

Two American Society for Testing and Materials (ASTM) groups, the ASTM WK62668 Detect and Avoid Performance Requirements Task Group and the ASTM WK62669 DAA Test Methods Task Group, are actively developing standards for sUAS DAA. The ASTM WK62668 DAA Performance Requirements Task Group has published a performance requirements standard (ASTM 2020). These performance requirements apply to Low Air Risk and Medium Air Risk operational volumes, which are operational volumes that are defined according to air collision risk. The defined categories are:

- High Air Risk: This is airspace where crewed aircraft predominately fly and/or the crewed aircraft encounter rate is frequent. The competent authority is expected to require the operator to comply with recognized DAA system standards as available and appropriate to the application.
- Medium Air Risk: This is airspace where crewed aircraft predominately do not fly (excluding helicopters and crop dusters) and/or the Crewed Aircraft (CA) encounter rate is occasional. This is generally uncontrolled airspace and/or airspace that extends from the ground to between 300 ft to 1,200 ft AGL (with 500 ft AGL used as a common default) above which most CA operations are conducted. This includes airspace away from Class B, C, D aerodromes, or near Class B, C, D aerodromes with additional strategic mitigations.
- Low Air Risk: This is airspace where crewed aircraft predominately do not fly (excluding helicopters and crop dusters) and/or the CA encounter rate is remote or improbable in accordance with guidelines from the competent authority. This is generally uncontrolled airspace and/or airspace that extends from the ground to between 300 ft to 1,200 ft AGL (with 500 ft AGL used as a common default) above which most crewed aircraft operations are conducted, and away from urban populations centers, towns, outer suburban, suburban, residential areas, metro, or cities, and outside all aerodromes.
- Extremely Low Air Risk: This is airspace where CA predominately do not fly and/or the CA encounter rate is extremely improbable. It is generally defined as airspace where the

risk of collision between a UAS and CA is acceptable without the addition of any tactical mitigation (e.g., a DAA system). An example of this may be UAS flight operations in some parts of Alaska or northern Sweden where the CA density is so low that it could meet the airspace safety threshold without any mitigation.

ASTM (2020) defined (logic) risk ratio performance requirements for Low Air Risk and Medium Air Risk operational volumes.[1] These are provided in Table 1.

Table 1. DAA performance guidance from ASTM (2020).

Intruder Equipage	NMAC (Near Mid-Air Collison) Risk Ratio (RR)	Well Clear Risk Ratio (LR)
Transponder or ADS-B Out	≤ 0.18	≤ 0.40
Non-Cooperative	≤ 0.30	≤ 0.50

2.1.2 Encounter Characteristics

From an encounter/trajectory standpoint, intruder aircraft can exhibit variations in the following (hereinafter four dimensions of variability):

- Horizontal direction
- Vertical direction (e.g., climb/descend)
- Horizontal speed
- Vertical speed/rate

These are generally considered to be ground-relative (e.g., ground-relative speed) and, of course, are components of the (ground-relative) aircraft velocity. By varying these, all types of encounter trajectories can be generated (straight, curved, curved with changes in horizontal speed, ascending, descending, curved with descent, etc.).

Traditionally, data regarding CA behavior has been characterized using encounter models (e.g., (Edwards et al. 2009; Griffith et al. 2013; Weinert et al. 2013; Underhill et al. 2018; Weinert et al. 2018). Such models have evolved such that aircraft characteristics are updated each second (Weinert et al. 2013). Given such models, typical flight patterns could be extracted, with any erratic (if present) and presumably less likely patterns not being used unless they represent a significant challenge for DAA systems. However, given the lack of CA data for very low-level flights (Weinert et al. 2019), such an encounter model does not exist. Weinert et al. (2019) is developing a model using ADS-B (Automatic Dependent Surveillance-Broadcast) data from the OpenSky network (Schäfer et al. 2014).

[1] Risk ratio is, generally, the likelihood of an event. In this context, the loss of well clear risk ratio, for example, is the ratio of the likelihood of the loss of well clear with use of a DAA system given an encounter set and the likelihood of loss of well clear without the use of a DAA system for that encounter set. See ASTM (2020).

Given that a statistical encounter model for crewed flight at very low levels is not available, a heuristic model based upon intruders that commonly operate at very low levels is used instead. Weinert and Barrera (2020) provide an extensive review of very low-level crewed operations. As indicated by Weinert and Barrera (2020), numerous crewed operations occur at very low levels, as shown in Table 2. Away from offshore areas, flight schools, specific tourist attractions, and urban areas (helicopter news and public safety), the most common operation is expected to be spraying and dusting.

Spraying and dusting operations consist of five types of flight "legs":

- Takeoff and landing
- Transition to and from the field being sprayed
- Application leg
- Ascent at the end of an application leg
- Descent into an application leg.

During the transition and application legs, the CA is generally in straight, level flight. During takeoff and landing, ascent at the end of an application leg, and descent into an application leg, the CA is ascending and descending and, during the last two legs, turning. Because a sUAS could encounter such an aircraft during any of these flight legs, testing of sUAS DAA systems should include both horizontal encounters and encounters where the intruder is approaching from above and below.

Table 2. Summary of very low-level crewed aircraft operations from Weinert and Barrera (2020).

Operation	Flight Altitudes (ft AGL)	Speeds (kts)	Comments
Spraying and Dusting	2-20	50-120	
Insect Release	300-2500	78-88*	
Fish Release	150-300	70	
Helicopter Air Ambulance	0 and up	Not Provided	
Helicopter Air Tours	400-3300	Not Provided	Aircraft models can be used to obtain airspeeds.
Helicopter Offshore Operations	500 and up	Not Provided	Aircraft models can be used to obtain airspeeds.
Training	500 and up**	Not Provided	Aircraft models can be used to obtain airspeeds.
Animal Sciences	30-4590***	19-175****	
Earth Sciences	100-2130	27-120	
Plant Sciences	<500-32,000	11-200	
Helicopter News and Public Safety	500-3280	0-140	

*Average speeds based on operational guidance.
**Based on regulations.
***Many operations are reported to occur below 500 ft AGL.
****175 kt flights at altitudes 1200-2000 ft AGL. Highest speed for altitudes < 700 ft AGL is 108 kts.

Away from offshore areas, flight schools, specific tourist attractions, and urban areas, helicopter air ambulance operations are arguably the second most common very low-level CA operation. While the exact altitudes at which such aircraft are flown when transiting to and from an accident site are not known, it is expected that such legs could be conducted at altitudes below 500 ft AGL and, by regulation [§135.203 of the Code of Federal Regulations (CFR)], 300 ft above the surface (e-CFR 2021a). In addition, such flights include ascent and descent in locations where encounters with sUAS may occur. Thus, both horizontal encounters and encounters where this type of intruder approaches from above and below are needed when testing sUAS DAA systems.

For the rest of the operations in Table 2, horizontal encounters with sUAS are expected to dominate the encounter set. It is noted that because helicopter air tours and helicopter news and safety flights can involve the CA hovering, such encounters include closure rates that are purely driven by sUAS flight speeds.

2.1.2.1 Geometries

During the prior set of flight tests conducted by the UND and NPUASTS in September 2020 (Askelson 2022), horizontal encounters including the full range of possible encounter angles (0°-360°) and using a 45° increment (0°, 45°, 90°, 135°, 180°, 225°, 270°, 315°) were conducted. Analysis of those tests indicated an interesting pattern in which the horizontal component of CPA (CPA_h) appeared to depend upon the encounter angle, with smaller CPA_h values associated with overtaking encounters (encounter geometries of 180° and 225°) and larger values associated with head-on encounters such as 0° and 45° [cf. Figure 22 of Askelson (2022)]. To explore whether the differences observed during the September 2020 flight tests consistently occur, the June 2021 tests utilized a selected subset of horizontal encounter angles (0°, 45°, 180°, 225°). In addition, for the horizontal encounters and these encounter angles, 10 tests at each angle were incorporated into the encounter test script (as opposed to 5 in the September 2020 test). Executing more tests at each angle produces greater confidence in observed differences and also enables exploration of dependence of statistical properties (e.g., variance) on the number of samples through comparison with previous test results. These horizontal encounters followed collision trajectories, wherein the aircraft were flown towards an Encounter Focal Point (EFP) using a vertical safety offset. This follows Askelson (2022), with the exception of a larger vertical safety offset of 400 ft [vs 350 ft with Askelson (2022)] used for this round of flight tests. Collision trajectories were used because they result in the strictest timing requirements for DAA for each encounter angle.

In addition to horizontal encounters, tests also included descend-into encounters, as shown in Figure 1. For these, horizontal origination points were the same as in horizontal encounters for the corresponding horizontal encounter angles, which were 0° and 135° for the June 2021 descend-into encounters. In these encounters, the intruder descended at a rate of 500 ft min^{-1} (a typical descent rate for the Piper Archer intruder aircraft used in this set of tests). Initial intruder altitude was set such that the intruder and UAS would fly to the same location, horizontally and vertically, without the use of the vertical safety offset (described subsequently). Thus, a collision-type geometry was employed and applied to the point of enacting the vertical safety offset. Given the horizontal 120 kt speed and 500 ft min^{-1} descent rate of the intruder, the vertical encounter angle is +2° (Figure 2).

Because ground features that could be used to ensure horizontal aircraft safety offsets were either not present or not aligned with horizontal encounter geometries, safety was maintained by having the intruder halt descent by the time 800 ft AGL was reached. Given that the UAS was operated at 390 ft AGL, this provided ~400 ft of vertical safety offset, which is 50 ft greater than that used in the September 2020 tests. With this design, at 900 ft AGL the intruder is ~250 ft from the vertical well clear boundary of the UA and, at a descent rate of 500 ft min^{-1}, ~30 s from the vertical well clear boundary. This produced a trend prior to activating the vertical safety offset that required a maneuver to maintain well clear in the vertical direction. In the horizontal direction, the trend is constant (before and after activation of the vertical safety offset) and required a maneuver to maintain well clear in the horizontal direction. Thus, the descend-into encounter design resulted in a trend to a well clear violation prior to activation of the vertical safety offset that required a maneuver for maintenance of well clear.

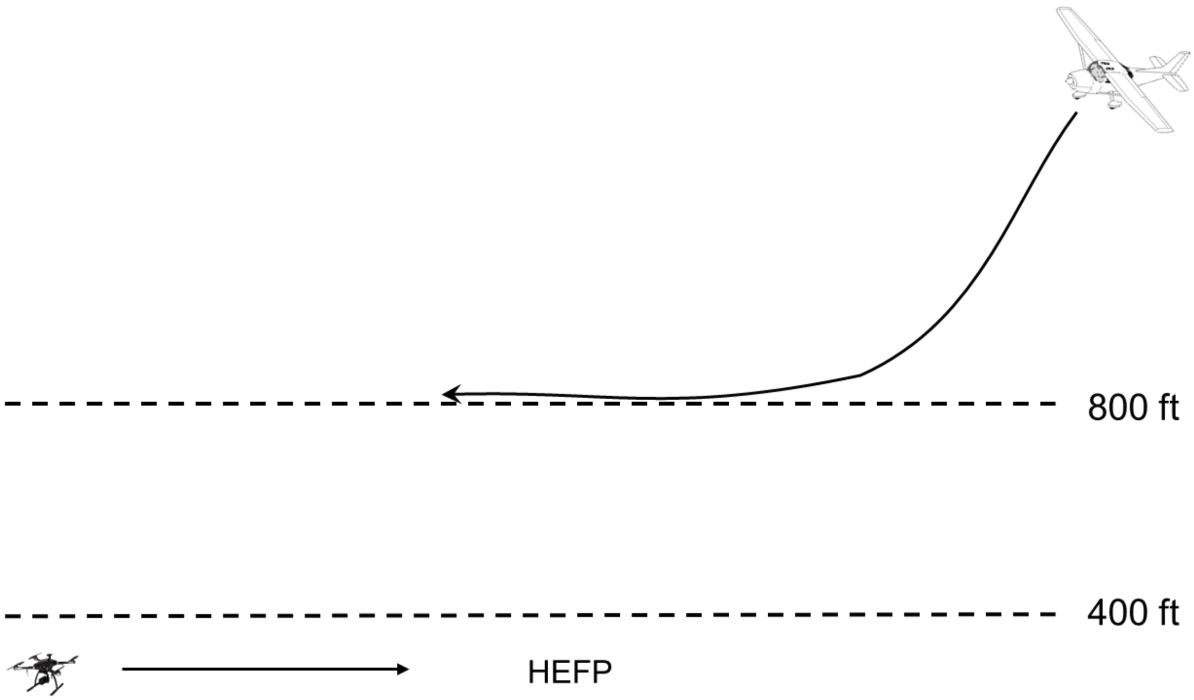

Figure 1. Illustration of descend-into encounters.

As in Askelson (2022), horizontal encounter angles are (clockwise) relative inbound course angles of the CA relative to the sUAS direction of travel as related to the EFP, as illustrated in Figure 2a. Thus, a horizontal angle of 0° is from the direction of sUAS track/heading (head-on). Vertical angles are elevations relative to the horizontal plane with the EFP as the reference point (Figure 2b).[2]

The encounter geometries used in the June 2021 tests include horizontal and vertical direction variations (two of the four dimensions of variability). They do not include all possibilities for these dimensions, however, as:

- They were straight-line encounters and thus did not involve any turns by either aircraft.
- They only included collision-type geometries (in the horizontal and vertical directions) and, thus, excluded encounters that would result in loss of well clear but not a collision (non-collision geometries).
- Only one vertical encounter angle (+2°), involving intruder descent, was tested.

2.1.2.2 Speed Variations

Speed variations were not included, with the desired intruder speed set at 120 kts for each encounter.

[2] It is noted that these are not the same as relative bearing, which is the angle measured clockwise from the heading of the UA to the location of the intruder, with the UA being the anchor point.

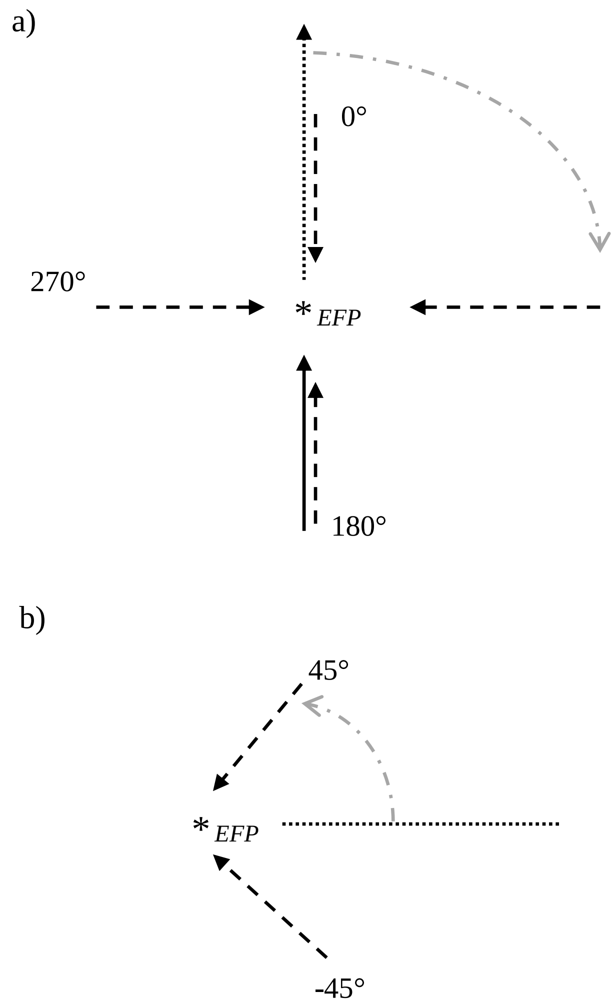

Figure 2. Illustration of encounter geometry angles in the horizontal and vertical planes. In a), the solid arrow indicates the flight path/course of the UA (Uncrewed Aircraft); dashed arrows indicate intruder flight paths/courses projected onto the horizontal plane, the dotted line indicates the reference for horizontal encounter angles, and the gray dash-dot line indicates the angle for the 90° horizontal encounter angle. In b), the flight path/course of the UA is into the page, dashed arrows indicate intruder flight paths/courses, the dotted line indicates the reference for vertical encounter angles, the gray dash-dot line indicates the angle for the 45° vertical encounter angle, and the intruder is assumed to approach the EFP from a 90° horizontal encounter angle for ease of illustration.

2.1.2.3 Considerations for LR

The June 2021 tests included the following variations:

- Horizontal direction variations

- Vertical direction variations

Variations that are not included are:

- Horizontal direction variations associated with:
    - Turns by either aircraft
    - Non-collision geometries
- Horizontal speed variations associated with:
    - Accelerations by either aircraft
- Vertical direction variations associated with
    - Non-collision geometries
- Vertical speed/rate

It is noted that this list of unincluded variations is subject to the following caveats:

- Maintaining a perfect heading while inbound to the EFP is not possible for either aircraft. These slight variations in heading had no discernable impact on the tests, as they had no apparent effect on identification of conflicts or on maneuvers.
- Establishing perfect timing such that both aircraft would arrive at the EFP at the same time is not possible. Consequently, the encounters were not perfect collision geometries.
- Maintenance of a constant speed while inbound to the EFP is not possible for either aircraft. Beyond potential impacts on the collision geometry (i.e., altering from a collision-geometry to a non-collision geometry), no impacts owing to these slight changes in horizontal speed were identified.
- Maintenance of constant altitude while inbound to the EFP during horizontal encounters is not possible for either aircraft. Observed variations in vertical direction and vertical speeds/rates had no discernable impact on identification of conflicts or on maneuvers.
- Maintenance of a constant intruder descent rate during descend-into encounters is not possible. No impacts owing to variations in intruder descent rate during these encounters were identified.

Use of data from these tests results in *LR* (well clear risk ratio) values that are different from those obtained by including all types of encounters. Addition of descend-into encounters is not expected to drastically alter values relative to horizontal-encounter-only tests given the use of Ground Based Detect And Avoid (GBDAA) and horizontal ownship maneuvers for maintenance of well clear (with these, avoidance is similar to that with horizontal encounters). Use of collision geometries is expected to generally produce larger *LR* values because they create the strictest timing requirements for each encounter geometry. Hence, if *LR* values are estimated from collision geometries then in general it may be expected that the values are larger compared to those estimated using a random distribution of encounter geometries. Exceptions occur when sensors used have poor track accuracy and any maneuver helps to prevent a collision when aircraft are on collision geometries. This approach only works when there is sufficient track accuracy to know how to maneuver with respect to an intruder and the maneuver strategy actually attempts to increase separation in contrast to strategies that hover or hold.

Another factor that impacts *LR* values is exclusion of horizontal encounter angles. For the horizontal encounters and 45° spacing, the 90°, 135°, and 270° horizontal encounter angles were excluded. For the descend-into encounters, the 45°, 90°, 180°, 225°, and 270° horizontal encounter angles were excluded. The impact of excluding these is unclear, although results from Askelson (2022) indicate that some dependence upon horizontal encounter angle exists, as shown in Figure 22 of that report. Other factors that impact *LR* values include use of linear trajectories (as opposed to curved trajectories for ownship and/or the intruder) and of constant horizontal and vertical speeds.

Because of these considerations, *LR* values herein are labelled with a modified symbol. The symbol $LR_{\subseteq c}$ is used, where the '$\subseteq$' indicates subset and the 'c' indicates collision geometries. Thus, this explicitly indicates that values are for a subset of the collision geometries.

A final important consideration is the limited number of samples that can be collected during flight testing. Risk ratios are commonly evaluated using a very large number (1000s or more) of simulations (e.g., ICAO 2014, §4.4.2.6; Deaton and Hansman 2019). In contrast, a week of flight testing will produce on the order of 100 encounters. Consequently, the risk ratio estimates obtained from flight tests have more sample uncertainty than do those from simulations. For this reason, risk ratio estimates obtained through flight testing are referred to herein as sample risk ratios.

2.2 Test Objectives

The objectives of the June 2021 flight tests were:

- Determination if the test methodology results in well-clear maintenance during encounters (especially with the increased vertical safety offset and for descend-into encounters)
- Collection of additional samples at selected horizontal encounter geometries and evaluation of impacts on statistical parameters

2.3 Test Personnel

Test partners are provided in Table 3. The UND and NPUASTS have been working with L3Harris™ Technologies for years and have developed a terrestrial UAS BVLOS capability that utilizes a C-Speed LightWave radar, Surveillance and Broadcast Services (SBS) ADS-B data, and Xtend™ ADS-B (L3Harris 2021) data. The L3Harris™ system includes visualization through the L3Harris™ RangeVue™ Pro system (L3Harris 2019). This display system was used as opposed to the RangeVue™ system used in the September 2020 tests, and did not have an Alerting and Guidance (A&G) capability at the time of the June 2021 tests.

Table 3. UND-NPUASTS June 2021 test partners.

Partner	Role
NPUASTS	Flight Test Coordinator, Technology Provider
UND	Project Coordination, Crewed Aircraft Intruder, Technology Provider
ISight Drone Services	UAS Operator
L3Harris™	Technology Provider

2.3.1 NPUASTS

The NPUASTS provided the Flight Test Director (FTD), who was based in the NPUASTS Operations Trailer, which was parked at the Lovas Farm (cf. §2.6). The FTD was the primary person leading the execution of the flight tests and oversaw operations using multiple data feeds and communicated directly with the flight teams via Stonecast radios, which utilize a radio tower network in northeast North Dakota (Stones Mobile Radio 2021). The NPUASTS provided Mission Commanders (MCs) to assist and ensure that flights adhere to NPUASTS Standards and Policy. The NPUASTS also provided data collectors and visual observers. The NPUASTS provided a suite of visualization, DAA, and data collection technologies in concert with the technology-providing partners on this project.

2.3.2 UND

The UND provided the data collection and analysis team, Principal Investigator (PI), intruder aircraft (Piper Archer), and Federal Aviation Administration (FAA) and press interface personnel. The PI interfaced with the FTD to ensure all goals were accomplished for the test event.

2.3.3 ISight Drone Services (UAS Operator)

ISight Drone Services flew the SuperVolo UAS. Isight Drone Services provided a flight crew (2-3 people), flight system, and spare batteries and parts.

2.3.4 L3 Harris Technologies

L3Harris™ provided a suite of GBDAA technology and UAS network infrastructure to support BVLOS operations. L3Harris™ collaborated with ISight Drone Services to integrate a data feed from the SuperVolo UA GCS (Ground Control Station) into the L3Harris™ DAA system at Hillsboro, ND, to provide ownship data to the L3Harris™ system. L3Harris™ also provided remote support for the system (including data collection).

2.3.5 Distribution and Roles

Personnel distribution, systems, and data sources for the core capabilities applied during the June 2021 tests are illustrated in Figure 3 (these are the same as for the September 2020 tests). The three primary operational locations were the Command Center Trailer, the Electronic Observer Trailer, and the UA Launch and Recovery Element (LRE). Each of these were at different locations: the Command Center Trailer was at the Lovas farm, the Electronic Observer Trailer was at the Hillsboro, ND, airport (co-located with the C speed radar), and the UA LRE was either at the Lovas farm or just across the coulee that passes south of the Lovas farm. More information regarding locations is provided in the Test Locations section.

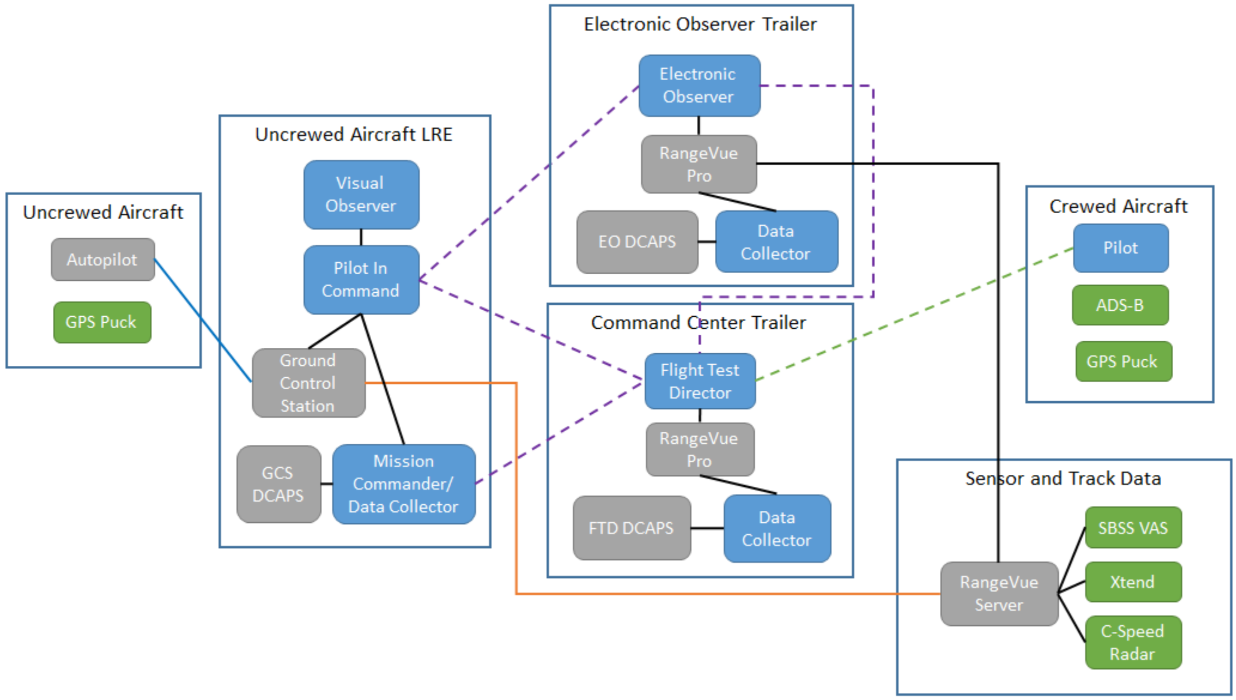

Figure 3. Personnel distribution, systems, and data sources for core June 2021 flight test capabilities. Personnel roles are shaded blue, systems are shaded grey, and data sources are shaded green. Communications/connections are indicated with lines, with solid black indicating a direct/wired connection, solid blue indicating the GCS-UA connection, solid orange indicating communcation via Long-Term Evolution (LTE), dashed green indicating communcations with the crewed aircraft via Very High Frequency (VHF) radios, and dashed purple indicating communications via Stonecast radios.

As indicated in Figure 3, data flow into the L3Harris™ system through what is labelled as "RangeVue Server". Details regarding this architecture are beyond the scope of this document. However, it is noted that multiple servers were being utilized, with the (Electronic Observer) EO RangeVue™ system receiving UA telemetry via Long-Term Evolution (LTE) to enable the EO to perform its functions. The RangeVue™ server acquires cooperative data from the L3Harris™ Surveillance and Broadcast Services Subsystem (SBSS) Value Added Service (VAS) and from local Xtend™ ADS-B units (L3Harris 2021). For the June 2021 tests, the RangeVue™ server collected noncooperative data from a C Speed Lightwave Radar (C Speed 2021). In addition, Global Positioning System (GPS) pucks, which are portable, self-powered GPS systems were utilized to collect truth data for aircraft position. The same type of GPS unit was used on both the UA and CA. An additional source of truth data for aircraft position is the ADS-B unit onboard the CA.

Systems illustrated in Figure 3 are:

- Command Center Trailer
    - RangeVue™ Pro: L3Harris™ DAA display system
    - Flight Test Director Data Collection And Processing System (DCAPS): A system that enables collection of DAA test data (described further in the Data Management section)
- Electronic Observer Trailer

  - RangeVue™ Pro: L3Harris™ DAA display system
  - Electronic Observer DCAPS: A system that enables collection of DAA test data
- Uncrewed Aircraft LRE
  - Ground Control Station: SuperVolo GCS
  - Ground Control Station DCAPS: A system that enables collection of DAA test data
- Uncrewed Aircraft
  - Autopilot: The SuperVolo autopilot
- Sensor and Track Data
  - RangeVue™ server: System that collects cooperative and noncooperative data and provides those to systems/displays.

Additional systems (beyond those illustrated in Figure 3) were utilized during the tests, including:

- Computers and network infrastructure: Throughout the system
- Xtend™ ADS-B: An Xtend™ unit was also utilized at the Command Center Trailer
- Weather Station: Used to monitor winds, etc., at the Command Center Trailer
- Simulyze: A data fusion and display system utilized by the NPUASTS
- Stratus 2 and SkyRadar DX: ADS-B units that provide data to Simulyze
- Digital Video Recorder (DVR) and Cameras: Video collection system in the Command Center Trailer for capturing operations (can capture video from both inside and outside of the trailer).

Communications were accomplished in several ways:

- Direct/Wired: Either direct (e.g., viewing a screen) or wired connections (solid black lines in Figure 3)
- Radio link for SuperVolo GCS-UA (solid blue line in Figure 3)
- LTE (solid orange line in Figure 3)
- VHF for FTD to crewed aircraft (dashed green line in Figure 3)
- Stonecast radios (dashed purple lines in Figure 3)

The roles illustrated in Figure 3 are:

- Command Center Trailer
  - Flight Test Director (FTD; NPUASTS): Primary person leading execution of the flight tests
  - Data Collector (NPUASTS): One data collector utilized the FTD DCAPS to collect flight test data. Another data collector recorded metadata (manual notes).
- Electronic Observer Trailer
  - Electronic Observer (NPUASTS): Monitored RangeVue™ Pro display and communicated maneuvers to UA Pilot in Command (PIC).
  - Data Collector (UND): Utilized the EO DCAPS to collect flight test data.
- Uncrewed Aircraft LRE
  - Visual Observer (ISight Drone Services): Assists the PIC with see and avoid function
  - PIC (ISight Drone Services): Person with final authority and responsibility for operation and safety of the UA

  - Mission Commander/Data Collector (NPUASTS): One person fulfilled this dual role of ensuring that flights adhered to NPUASTS Standards and Policy and utilizing the GCS DCAPS to collect flight test data.
- Crewed Aircraft
  - Pilot (UND): Operated the crewed aircraft

A high-level overview of the testing process is provided in Appendix A and illustrated in Figure A1. Example test cards for scenario DE_0_2_120 [Descend-into Encounter (DE) with a 0° horizontal encounter angle, 2° vertical encounter angle, and 120 kt intruder speed] are provided in Appendix B. As shown in these cards, the sequence of events is summarized as:

- The CA and UA move to their stand-off (starting) locations
- The CA starts inbound to the EFP
- The FTD director directs the UA to begin its inbound leg to the EFP
- Events such as first detection, track initiation, etc., are recorded
- The EO determines if a conflict exists
- If the EO determines that a conflict exists, the EO identifies and maneuver and instructs the PIC to maneuver
- The FTD declares end of encounter

Additional types of data (e.g., time of closest point of approach) are collected by data collectors. The FTD coordinates events such as UA and CA launch and recovery.

2.4 DAA System

Testing was conducted using the L3Harris™ Technologies DAA system with the RangeVue™ Pro display system, which did not provide A&G and thus had one option for the Evaluate component of DAA.[3] Table 4 provides information regarding this instantiation of the L3Harris™ DAA System.

[3] In the related research effort that preceded this effort, Askelson et al. (2017) identified the major steps in DAA as Detect, Track, Evaluate, and Maneuver (DTEM). These are defined as Detect—sense the presence of something for which avoidance may be needed; Track—estimate the path of the intruder; Evaluate—determine whether identified intruders pose a threat, prioritize threats, and identify maneuver; Maneuver—execute maneuver. These map to the functions in ASTM (2020) according to: Detect Function DF (Detect and Track), Alert Function A1F (portion of Evaluate wherein hazards are identified and prioritized), and Avoid Function A2F (portion of Evaluate where the maneuver is identified and Maneuver).

Table 4. Information regarding the L3Harris™ DAA system used during the June 2021 tests.

DAA Step	DAA Steps	Description
Detect	C-Speed Lightwave Radar and ADS-B (SBSS VAS and Xtend)	Detect data for non-cooperative targets are provided using a C Speed Lightwave Radar. Data for cooperative targets are provided through the SBSS (VAS and through Xtend ADS-B units.
Track	Best-source selection	Data having the most accurate information regarding intruder locations/tracks are used. Track data are provided through the SBSS VAS or by the C-Speed Lightwave Radar.
Evaluate	EO (Electronic Observer)	The EO performs the functions in this step. The display system is RangeVue™ Pro and ownship data are ingested into the system through a telemetry feed from the UAS GCS.
Maneuver	Human Pilot	The SuperVolo flight crew executed maneuvers once received from the EO. This involved setting new waypoints for the SuperVolo.

The L3Harris™ Technologies DAA system obtains intruder detection data from several sources. Non-cooperative data are provided using a C Speed Lightwave Radar (C Speed 2021; Figure 4). This is a low-cost, flexible, "software-defined", S-Band, two-dimensional (2D) radar technology platform that can serve a broad range of surveillance missions through reconfiguring of its run-time parameters. Cooperative data are obtained from the L3Harris™ SBSS VAS and from local Xtend™ ADS-B units (L3Harris 2021) that act as gap-fillers to provide surveillance coverage in areas that may not be effectively covered by the FAA's system (provided through the SBSS VAS).

Figure 4. The C Speed Lightwave Radar utilized during the June 2021 flight tests.

Track data are provided by the L3Harris™ SBSS VAS (cooperative intruders) and the C Speed Lightwave Radar system. The L3Harris™ system performs a best source selection. Thus, it selects the surveillance source that provides the best information regarding an intruder and displays those data (locations and tracks). Generally, the source that provides the lowest uncertainty regarding intruder location is considered to be the best source. Therefore, these flight tests generally utilized a cooperative DAA system. This, however, had no negative impacts on test objectives.

For the Evaluate step, the EO used the RangeVue™ Pro display to identify conflicts and identify maneuvers, and a Stonecast radio to communicate maneuvers to the UA PIC. In the absence of an A&G system, distance-based circles were drawn around the UA, as illustrated in Figure 5. The radii of these (outer) circles are generally equal to the horizontal extent of the hazard zone as defined by RTCA (2017; §2.2.4.3.2), which vary with horizontal encounter geometry to account for changes in closure rates and depends upon the alert threshold. For these tests, a late (60 s) alert threshold was used to limit the distance between UA origin points and the EFP, which simplified Part 107 operations in that daisy-chained ground observers were not required and sped up the testing process by decreasing the amount of time required for set-up between encounters. For simplicity, distances for 0° and 180° horizontal encounter angles were computed, and distances for intervening angles were linearly interpolated from those values. In addition, a buffer of 0.17 mi was added for 180° encounters, which provides an additional 5 s. This was based upon computations of the amount of time required for the UA to travel 2000 ft [the horizontal well-clear distance used in ASTM (2020)] from the line adjoining the aircraft tracks for a 180° encounter, the estimated amount of time required for initiating a maneuver (~15 s), and the distance the intruder travels in that amount of time.

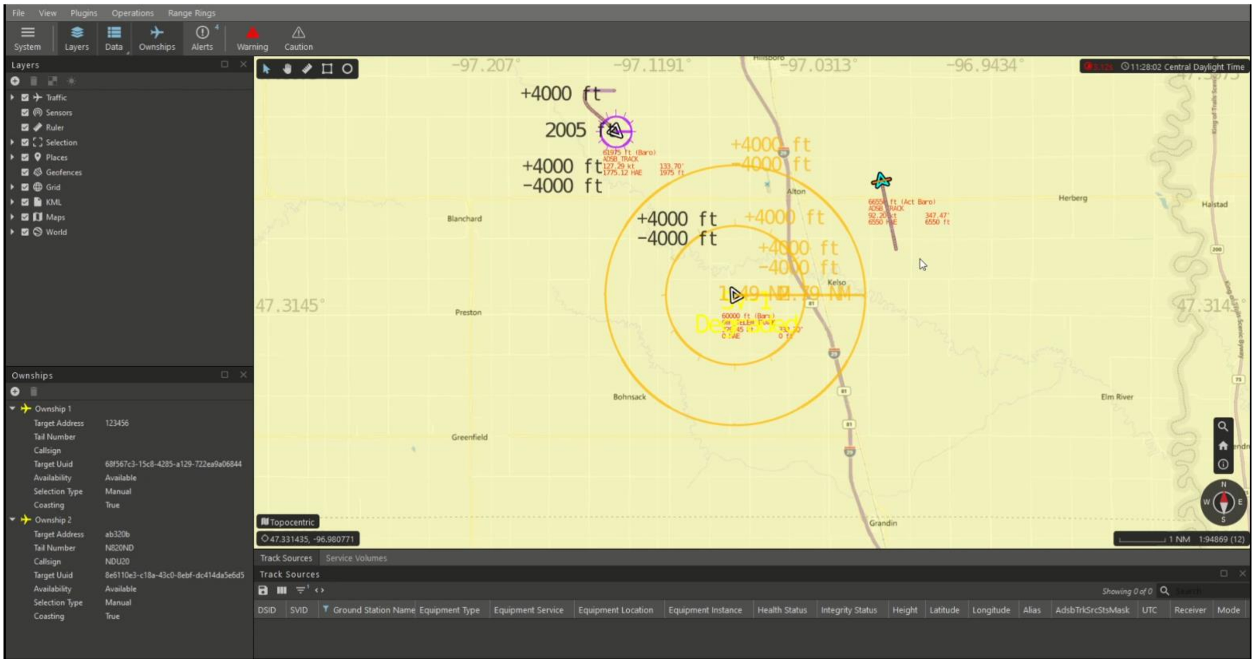

Figure 5. Example of the RangeVue™ Pro display. The UA is indicated by the triangle symbol located near the center of the display, with concentric rings drawn around it. The intruder is indicated by the triangle symbol surrounded by a magenta-colored circle. The outer ring around the UA serves as the alert for the EO to identify and communicate a maneuver to the UA PIC.

Maneuvers were executed by the UA PIC. Callbacks of commanded maneuvers were commonly used for acknowledgement.

2.5 Test Aircraft

The UA that was flown is Isight Drone Services' SuperVolo UAS. Specifications for the SuperVolo are provided in Table 5.

The Piper Archer intruder aircraft is owned by UND and was operated by UND during the June 2021 flight tests. Information regarding this aircraft is provided in Table 6.

Table 5. Information regarding the UA used during the June 2021 flight tests.

	The SuperVolo is a long range, Vertical Take-Off and Landing (VTOL) UAS designed for simplified deployment/ease of use. It utilizes a hybrid gas/electric power plant. The SuperVolo enables quick refueling for successive flights and requires very little ground infrastructure for operations. It also features a modular airframe that enables diverse payload configurations and cost-effective maintenance.		
Wing Span	3.0 m	**Cruise Speed**	18-34 m s^{-1}
Maximum Takeoff Weight	18.2 kg	**UAS Operator**	ISight Drone Services
Endurance	8 hrs	**GCS Type**	ACER computer with Swift GCS
Autopilot	CUAV PixHawk – Mavlink		

Table 6. Information regarding the intruder aircraft used during the June 2021 flight tests.

	The Piper Archer is a two-seat, tricycle-gear general aviation airplane that is used heavily in UND's aviation education and training programs.		
Wing Span	35 ft 6 in	**Cruise Speed**	128 kts
Maximum Takeoff Weight	2,550 lb	**Operator**	UND
Fuel Capacity	50 US gal		

2.6 Test Locations

2.6.1 Locations of Test Elements

The Command Center Trailer illustrated in Figure 3 was located at the Lovas Farm, at approximately (-97.082223, 47.329763). One UA LRE was at approximately (-97.084370, 47.329733), which is at the Lovas Farm and very near the Command Center Trailer, and the other UA LRE was at approximately (-97.090454, 47.327013). The DAA system, C Speed radar, and Electronic Observer Trailer were located on the ramp of the Hillsboro, ND, airport at (-97.061847, 47.357982). The Hillsboro airport is approximately 1.8 NM northeast of the Lovas Farm. For reference, the EFP was at (-97.087696, 47.328505). The locations of the Command Center Trailer, one UA LRE, and the Electronic Observer Trailer are illustrated in Figure 6.

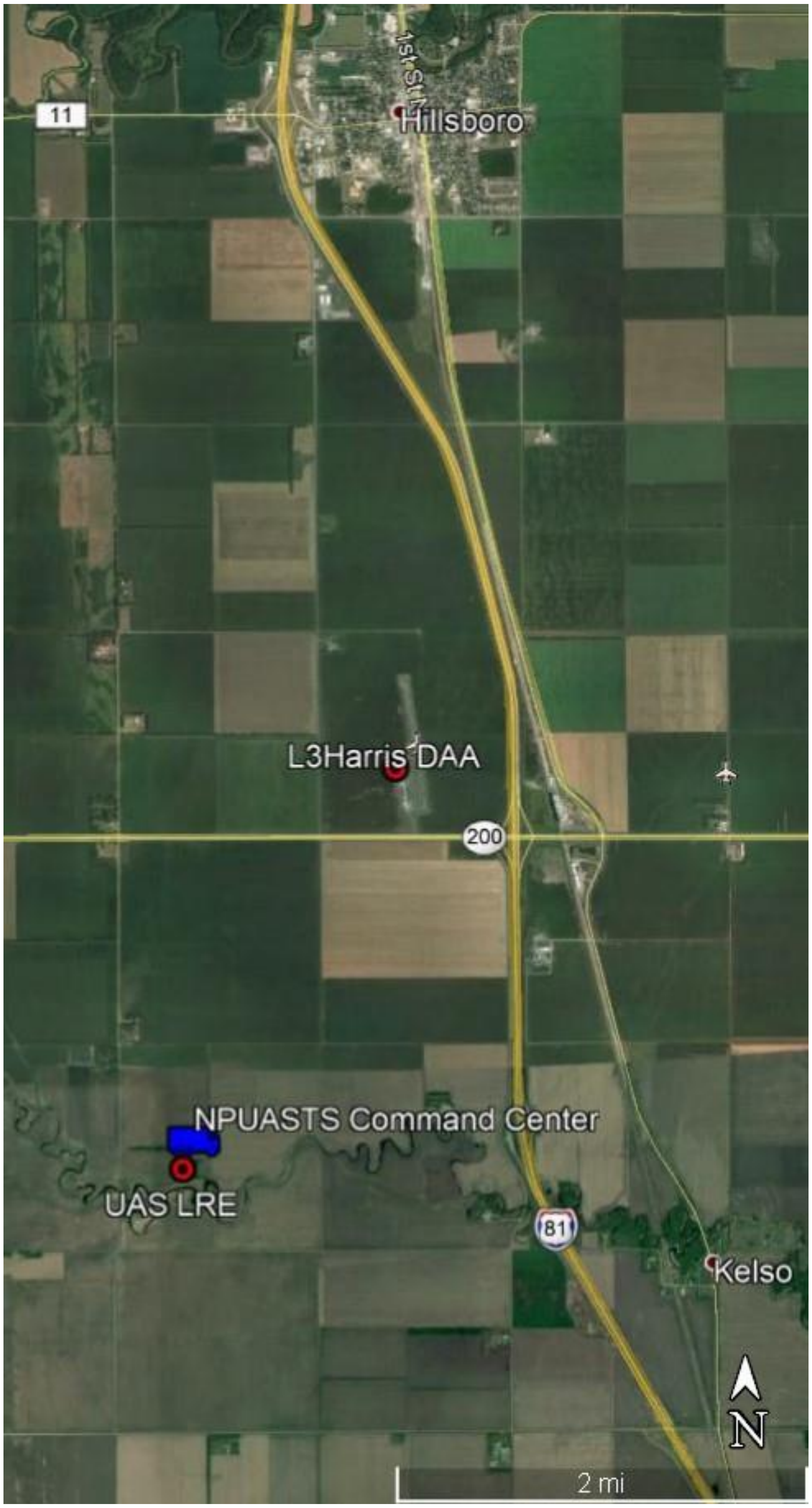

Figure 6. Locations of testing elements during the June 2021 flight tests.

The UA was flown to the southwest of the Hillsboro airport to avoid any issues with the airport. The crewed aircraft launched from the Grand Forks International Airport (KGFK) and refueled at the Hillsboro Airport (3H4) as needed. Figure 7 provides a sectional chart for the area. The test area is Class G airspace up to 700 ft AGL (Above Ground Level) and Class E airspace above 700 ft AGL (up to Class A airspace).

Figure 7. Sectional centered on the June 2021 flight test area.

Figure 8 provides images from the Lovas Farm, the location of the Command Center Trailer and one UA LRE. That UA LRE was approximately in the location of the large snowbank near the barn shown in the upper-right panel of Figure 8. Flights tests were conducted to the south and west of the Lovas Farm.

Figure 8. Images from the Lovas farm, the location of the Command Center Trailer and one UAS LRE. View is to the north (upper-left), to the east (upper right), to the south (lower left), and to the west (lower right).

2.6.2 Georeferenced Encounter Geometry Generation

The five horizontal encounter angles [0°, 45°, 180°, and 225° for Horizontal Encounters (HEs) and 0° and 135° for DEs] were generated by having the CA fly the same path either northwest to southeast or southeast to northwest and by varying the UA origination point. The two scenarios for CA flight direction are illustrated in Figures 9 and 10. The encounter geometries associated with UA origination points for the CA flying northwest to southeast (Figure 9) are:

A. 180°
B. 225°
E. 0°

The encounter geometries associated with UA origination points for the CA flying southeast to northwest (Figure 10) are:

B. 45°
D. 135

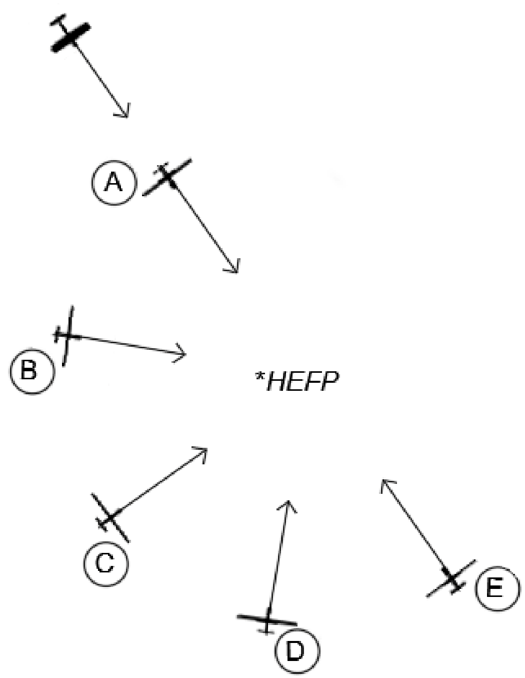

Figure 9. Illustration of encounters associated with the CA flying northwest to southeast. The top image illustrates aircraft paths and origination points. The bottom figure provides labels for UA orignation points.

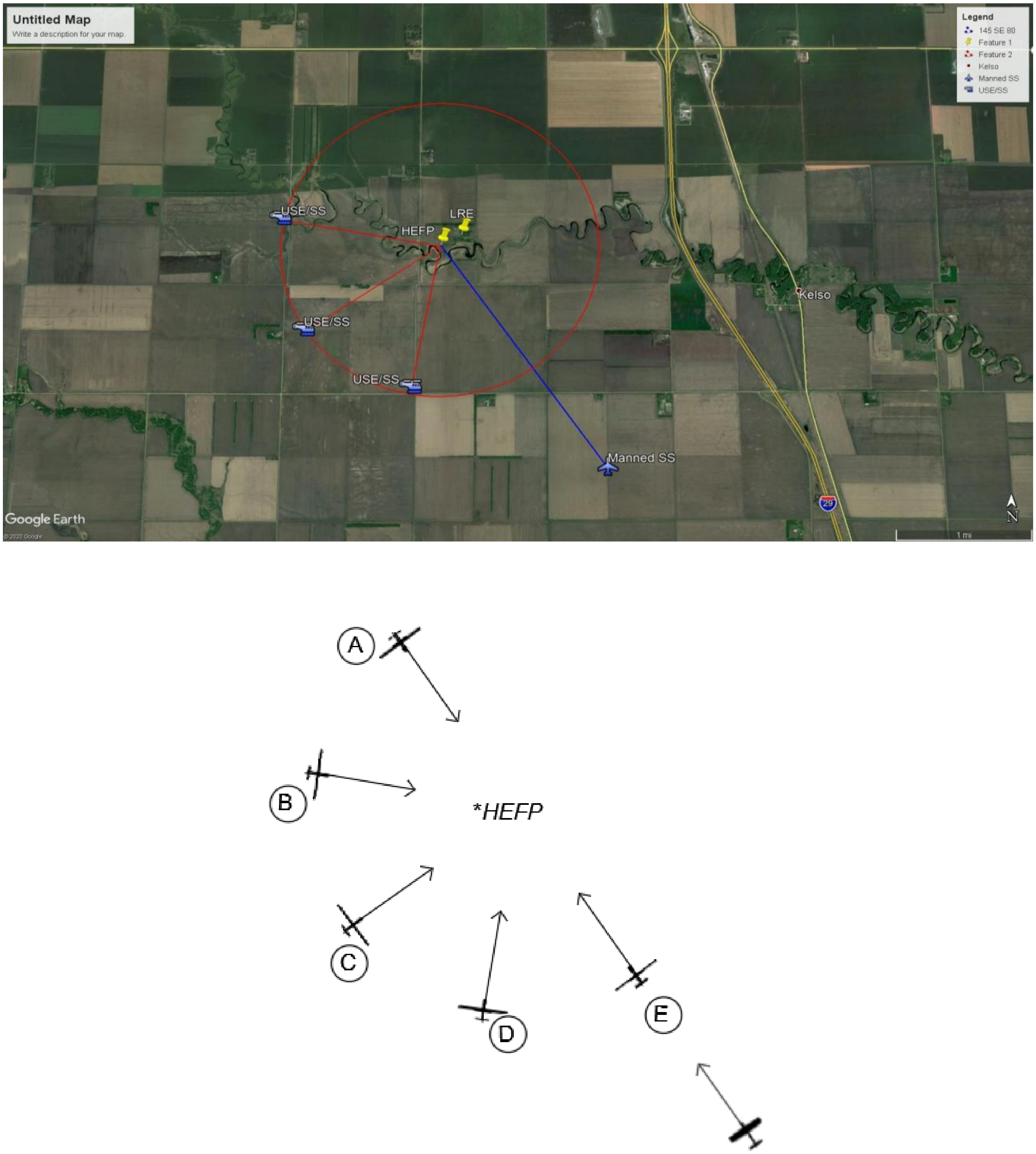

Figure 10. As in Figure 9 but for the CA flying southeast to northwest.

2.7 Test Dates and Schedule

Tests were conducted during the week of 13-19 June 2021. 14 June 2021 was a planned shakedown day. The team encountered challenges with provision of UA location data to the L3Harris™ system. These issues were resolved on the afternoon of 15 June, resulting in three test days: 16-18 June 2021. The planned schedule for that week is provided in Figure 11.

Start	End	Day 1: 15 June 2021	Day 2: 16 June 2021	Day 3: 17 June 2021	Day 4: 18 June 2021
600	630				
630	700				
700	730	Meet at NPUASTS (4201 James Ray Dr.)	Meet at NPUASTS (4201 James Ray Dr.)	Meet at NPUASTS (4201 James Ray Dr.)	Meet at NPUASTS (4201 James Ray Dr.)
730	800	Travel to Site	Travel to Site	Travel to Site	Travel to Site
800	830	Morning Briefing	Morning Briefing	Morning Briefing	Morning Briefing
830	900	Site Setup and Preparation	Site Setup and Preparation	Site Setup and Preparation	Site Setup and Preparation
900	930				
930	1000	Flight Testing	Flight Testing	Flight Testing	Flight Testing
1000	1030				
1030	1100				
1100	1130				
1130	1200				
1200	1230	Lunch and Aircraft Refueling	Lunch and Aircraft Refueling	Lunch and Aircraft Refueling	Lunch and Aircraft Refueling
1230	1300	Flight Testing	Flight Testing	Flight Testing	Flight Testing
1300	1330				
1330	1400				
1400	1430				
1430	1500				
1500	1530				
1530	1600				
1600	1630	Site and Equipment Tear Down	Site and Equipment Tear Down	Site and Equipment Tear Down	Site and Equipment Tear Down
1630	1700				
1700	1730	Debrief and Schedule Review	Debrief and Schedule Review	Debrief and Schedule Review	Debrief and Schedule Review
1730	1800				
1800	1830	Travel to NPUASTS	Travel to NPUASTS	Travel to NPUASTS	Travel to NPUASTS

Figure 11. Planned test schedule for June 2021.

2.8 Test Conditions

Weather conditions for flight tests conform to Part 107 requirements (e-CFR 2021b) since the SuperVolo was operated under Part 107. No notable challenges regarding electromagnetic interference were identified prior to or during testing.

2.9 Test Cards

Test cards were developed for three roles: FTD, UA pilot, and CA pilot. A total of 18 cards [(4 HE scenarios + 2 DE scenarios) x 1 intruder speed x 3 roles] supported this test campaign. Example test cards are provided in Appendix B. In addition to encounter type (HE and DE), values that changed in test cards are associated with the origination points of the UA and CA. The origination points for the UA and CA are provided in Table 7.

Table 7. Origination points for the UA and CA used during the June 2021 flight tests.

Aircraft	Speed	Origination Point	Longitude (°)	Latitude (°)
Crewed	120	NW	-97.126405	47.365509
Crewed	120	SE	-97.049435	47.288497
Uncrewed	120	A	-97.100994	47.340676
Uncrewed	120	B	-97.110610	47.331095
Uncrewed	120	D	-97.091593	47.312440
Uncrewed	120	E	-97.075449	47.315149

Test cards were reviewed by the UND/NPUASTS team, the broader A18 team, and the FAA prior to execution. A key to ensuring safety was use of a 400 ft vertical aircraft offset (50 ft larger than used during the September 2020 tests) during the execution of these encounters.

2.10 Data Collection and Management

2.10.1 Metadata

Metadata regarding the executed tests were collected. These data were generally collected using a spreadsheet like that illustrated in Figure 12. Metadata were also collected by various participants in the form of hand-written notes. These include notes collected by the FTD and by the data collector in the Electronic Observer Trailer.

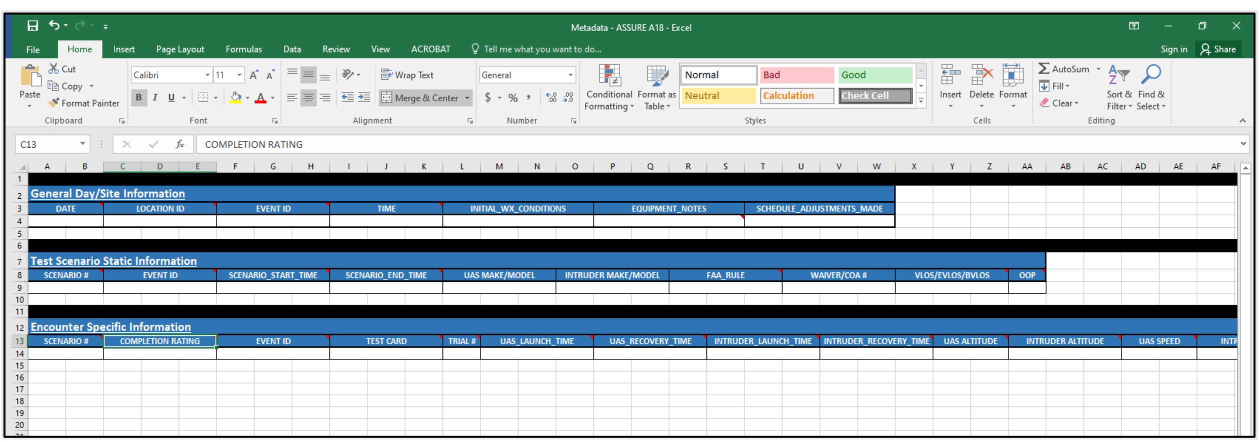

Figure 12. Spreadsheet utilized to capture test metadata.

2.10.2 DCAPS

The DCAPS was used to collect data regarding events that occurred during testing. DCAPS was developed by an L3Harris™ partner during previous research projects and provides a very convenient means for collecting DAA test data. Within DCAPS, different roles (e.g., data collector at the Electronic Observer Trailer) with associated events are defined. These events are presented as buttons. Selection of these events/buttons results in recording of the event, time, and origination station for that record. Numerous DCAPS stations can be active during a test, with the data stored in a combined file. In addition, comments can be added by users to collect notes. DCAPS interfaces for the GCS, EO, and FTD are shown in Figures 13-15.

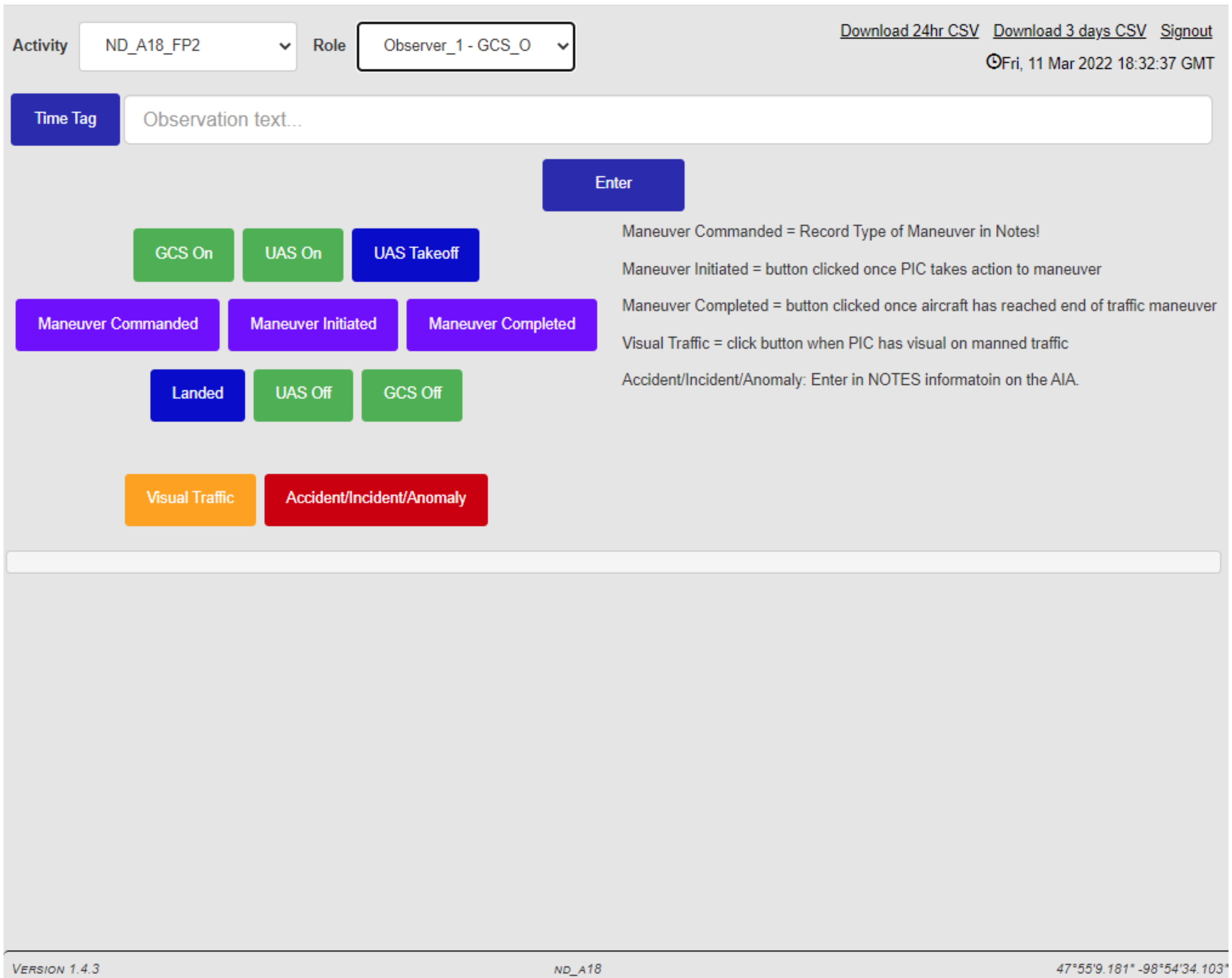

Figure 13. GCS DCAPS interface.

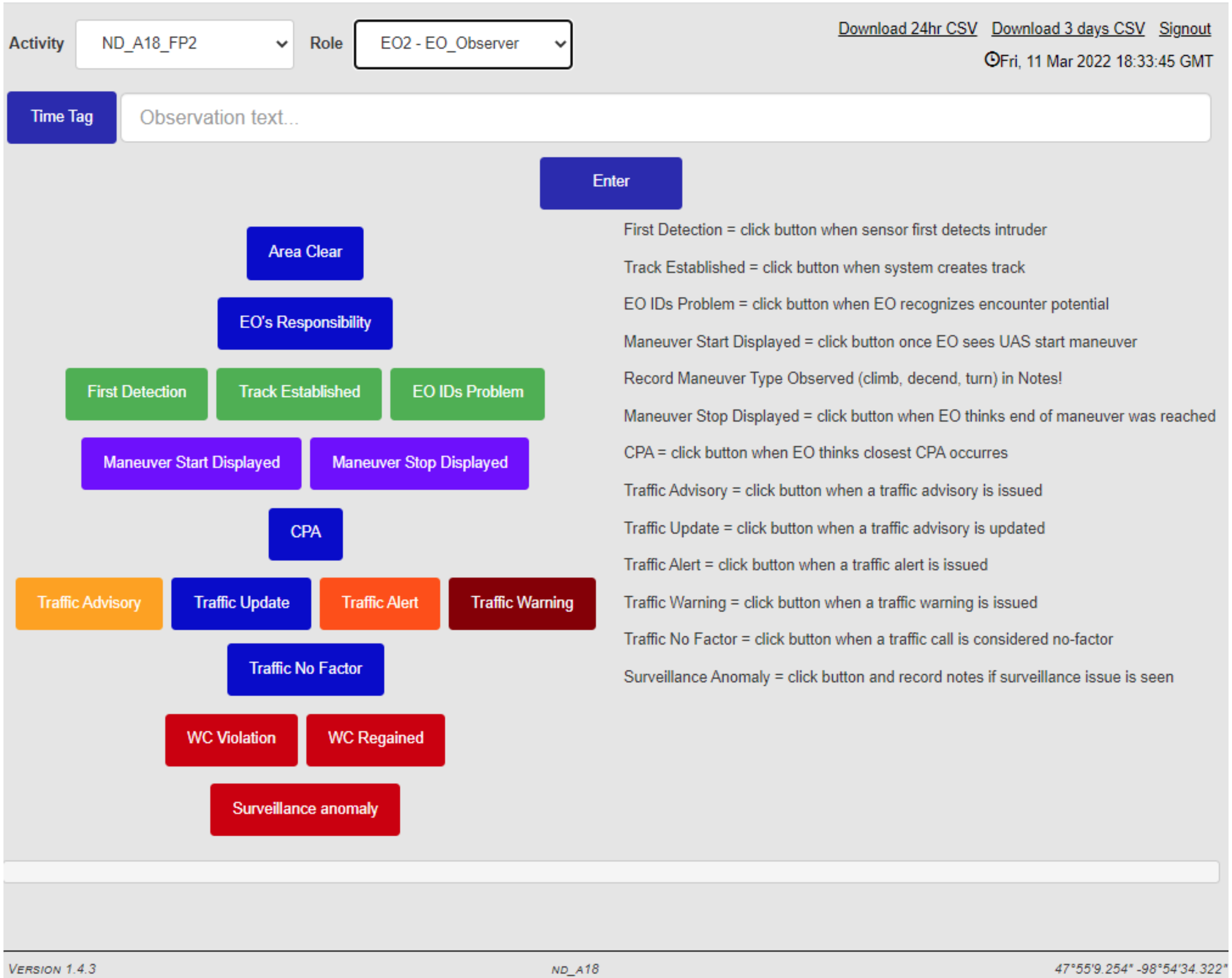

Figure 14. EO DCAPS interface.

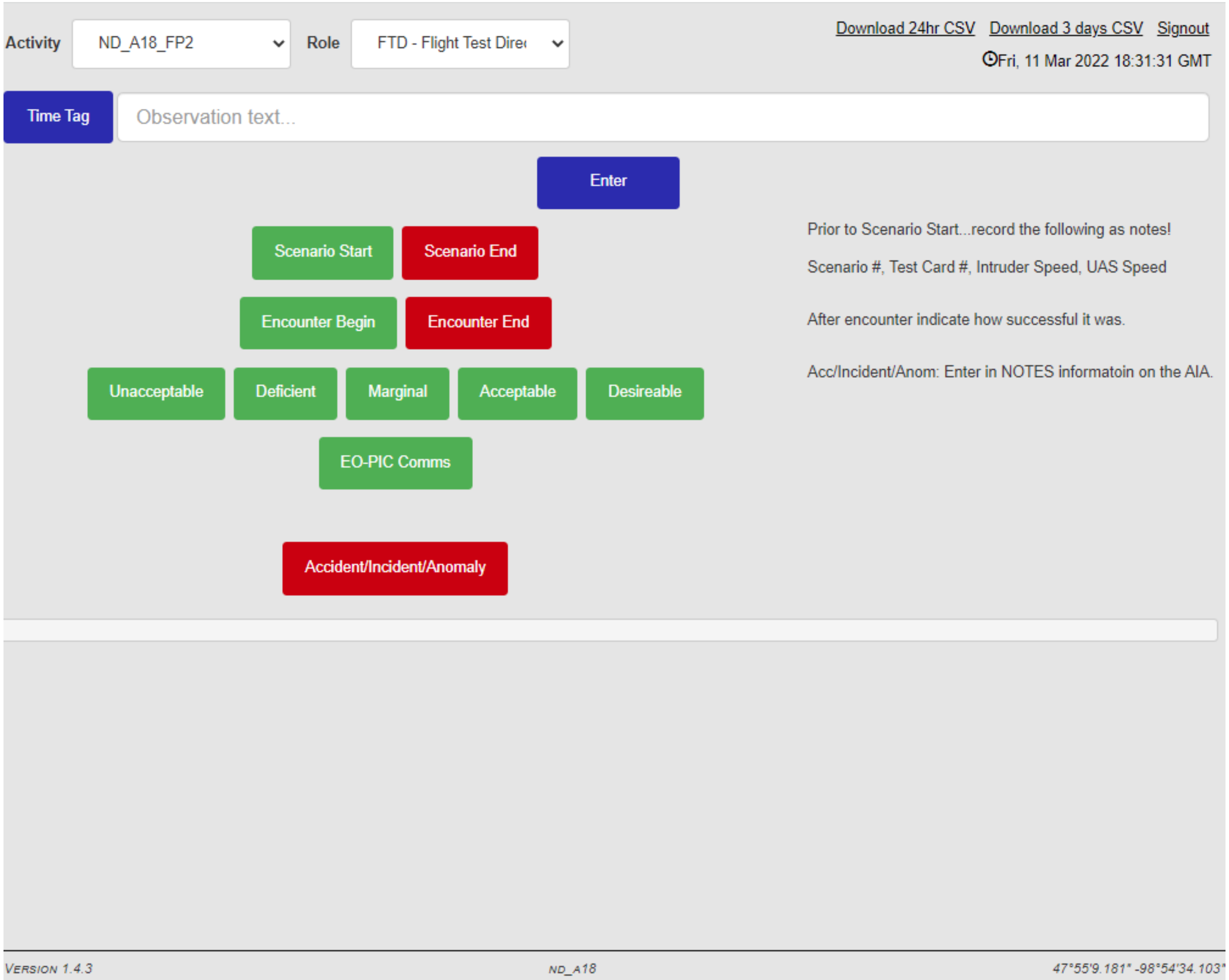

Figure 15. FTD DCAPS interface.

2.10.3 Aircraft Position Truth Data

For both the UA and CA, aircraft position data were collected using Qstarz BT-Q1000XT GPS pucks (Qstarz 2021). These self-powered pucks are very easy to use, being activated with a single switch. The data are, by default, enhanced by the Wide Area Augmentation System (WAAS) (USDOT 2021). This system improves location accuracy by decreasing horizontal and vertical position errors to roughly ½ and ¼ of those produced by Standard Positioning Services (SPSs), respectively. As indicated in Table 8, errors for Minneapolis, which is the closest station provided by FAA William J. Hughes Technical Center (2021), are ≤ ~1 m in both the horizontal and vertical directions 95% of the time, indicating that the aircraft position truth data utilized in these tests are expected to be very accurate. The data from FAA William J. Hughes Technical Center (2021) are for the period 1 July – 30 September 2021.

Table 8. GPS errors from Table 2-1 of FAA William J. Hughes Technical Center (2021).

Location	WAAS 95% Horizontal (m)	WAAS 95% Vertical (m)	SPS 95% Horizontal (m)	SPS 95% Vertical (m)
Average of 38 Locations	0.67	1.1	1.64	3.4
Minneapolis	0.626	1.035	1.49	3.15

In addition to data collected with the Qstarz BT-Q1000XT GPS pucks, CA ADS-B data and UA flight log data were also collected.

2.10.4 Additional Data Sets

Additional data were collected during the test period. These include:

- C-Speed Lightwave Radar: Data from the C-Speed Lightwave Radar were collected and stored.
- RangeVue™: Data handled with the RangeVue™ system are logged by L3Harris™. This includes FAA ADS-B and radar data provided by SBSS VAS.
- Xtend™ ADS-B: An Xtend™ unit was also utilized at the Command Center Trailer.
- Stratus 2 and SkyRadar DX: ADS-B units that provide data to Simulyze.
- Weather Station: Used to monitor winds, etc., at the Command Center Trailer.
- DVR and cameras: Video collection system in the Command Center Trailer for capturing operations (can capture video from both inside and outside of the trailer).

3 DATA ANALYSIS

3.1 Metrics

Results from this set of flight tests are organized according to individual encounters and the overall test campaign. Except where noted, the following is as in Askelson (2022).

3.1.1 Individual Encounter Metrics

3.1.1.1 Encounter Events

Encounter events that are captured are related to well clear status. These are:

- Well clear violation
- Horizontal well clear violation
- Vertical well clear violation

Well clear violations occur when the vertical aircraft safety offset failed to maintain vertical well clear status and the DAA operation failed to maintain horizontal well clear status. A horizontal well clear violation occurs for these horizontal (type) encounters when the DAA operation failed to maintain horizontal well clear status and the vertical aircraft safety offset enabled maintenance of vertical well clear status. A vertical well clear violation occurs when horizontal well clear is maintained but vertical well clear is not maintained.

Tracking vertical well clear violations assists with evaluation of the efficacy of the vertical aircraft safety offset. However, vertical well clear violations can happen during segments of encounters that are not relevant. This includes the beginning and end of encounters when aircraft may be maneuvering to set-up the next encounter, landing, etc. Thus, vertical well clear violations are only identified if they occur during the Objective Encounter Period (OEP), which is defined in the next section.

The speed of the SuperVolo commonly resulted in the UA reaching the visual range limit associated with Part 107 prior to the time when aircraft separation was minimized. Once at that limiting range, the aircraft was directed to station-keep (fly circles around a defined location). To obtain results consistent with a BVLOS type of operation in which such station-keeping would not generally occur, the straight-line portion of the UA path associated with its maneuver was extrapolated forward/coasted.[4] This results in the possibility of some sort of well clear violation occurring during the coasted period. Thus, events are reported during both the non-coasted and coasted periods.

3.1.1.2 Encounter Descriptors

Qualities that define portions of the encounters are used to enable analysis. The first is the beginning and end of the inbound (to the EFP) portions of flight paths for both aircraft. An aircraft is inbound (to the EFP) when the following are realized:

- Projection of the position of the aircraft ahead, using its current heading, the distance it is from the EFP is within a certain distance of the EFP.
- Distance to the EFP is decreasing.
- An aircraft is not maneuvering.

All encounters were examined to determine the tolerance distance relative to the EFP (first condition above). A tolerance distance of 2500 ft was used. While aircraft generally would pass much closer to the EFP if no maneuvering occurred, occasionally the CA would miss the EFP by distances that approached 0.5 miles.

The last criterion in the above list is whether the aircraft is maneuvering. Because CA paths are predefined to pass through the EFP (horizontally) and UA actions/maneuvers are of interest, maneuvers were identified only for the UA.

Analysis of GPS puck data provides maneuver information through use of flags that indicate if the aircraft turned or climbed/descended. In addition to these, the type of turn or whether the aircraft was climbing/descending is indicated according to:

- Turn type:
  - R: Right
  - L: Left
- Climb/descent:
  - C: Climb
  - D: Descend

---

[4] A means for estimating the amount of time for which coasting is computed was not developed. Instead, a fixed coasting period of 60 s was applied.

A three-dimensional maneuver involving both a turn and climb/descent can be identified using the combination of variables for turning and climb/descent. It is noted that the software does not currently properly label maneuvers in which an action is suspended (e.g., suspension of descent). Such maneuvers are identified, but are given a potentially-misleading label (suspension of descent, for instance, would be labelled as ‘C’).

Both turning and climb/descents are identified using differences between data that have been smoothed using a running average of length 3. Such smoothing was applied to eliminate false indications of turns or climbs/descents that arise owing to small-scale variations in aircraft position caused by turbulence, GPS errors, etc. Turns are identified when the current turn rate (after application of running average) differs from the previous turn rate at the previous GPS puck position (after application of running average) by 7 deg s^{-1}. This value was derived by examining turn rate differences during the OEP for all satisfactory encounters that were executed during the September 2020 test campaign (Askelson 2022).

Climbs or descents are identified in a similar manner using differences in climb/descent rates for data smoothed using a running average of length 3. Currently, the threshold for identifying climbs/descents is 7 ft s^{-1}. ASTM (2020) states that a nominal climb/descent rate for when vertical direction indicators are needed for intruders is 8.33 ft s^{-1}. ASTM (2020) also states that a low UA vertical agility is associated with 4.167 ft s^{-1} and a high UA vertical agility is associated with 8.33 ft s^{-1}. It is noted that since these tests did not involve vertical CA maneuvers, data from these tests were not useful for identifying vertical maneuver thresholds. Thus, the threshold used in the software may need to be modified for tests that involve vertical maneuvers.

The beginning of the UA maneuver period is identified by searching for a maneuver that occurs after the beginning of the inbound portion of the UA flight path. The end of the maneuver is defined, for tests such as these in which well clear maintenance is through horizontal UA maneuvers, as:

- If a well clear or horizontal well clear violation occurred, the time when well clear or horizontal well clear was regained.
- If neither a well clear nor horizontal well clear violation occurred, the time when the horizontal distance between aircraft begins to increase.

Another important period during an encounter is the OEP. This is the period within an encounter when the two aircraft are deemed to be interacting and is, then, the relevant period of an encounter. It is defined by:

- Beginning: The earliest time when both aircraft are inbound to the EFP.
- End: The earliest of either the declared end of encounter (from DCAPS data) or when the horizontal distance from the well clear boundary exceeds 2000 ft and the horizontal distance between aircraft is increasing with time.

The condition of being 2000 ft beyond the horizontal well clear boundary was chosen because at that distance the unmitigated Near Mid-Air Collision (NMAC) risk is reduced to approximately half of its value that occurs at the horizontal well clear distance (Weinert et al. 2018).

An additional encounter descriptor that was not used in the analysis of the September 2020 test data (Askelson 2022) was added. This is the coasted period, which provides extrapolated position estimations for the UA based upon the straight-line portion of its path during its maneuver.

3.1.1.3 Distance Metrics

One distance metric that is used is distance to the well clear volume, d_{wc}, which quantifies how near one came to a well clear violation and the severity, from a distance perspective, of a well clear violation. This metric is given by

$$d_{wc} = \begin{cases} \sqrt{h_{wc}^2 + v_{wc}^2} & h_{wc} > 0 \text{ and } v_{wc} > 0 \\ h_{wc} & h_{wc} > 0 \text{ and } v_{wc} < 0 \\ v_{wc} & v_{wc} > 0 \text{ and } h_{wc} < 0 \\ h_{wc} \text{ or } v_{wc} & h_{wc} < 0 \text{ and } v_{wc} < 0, \end{cases} \quad (1)$$

where h_{wc} and v_{wc} are the horizontal and vertical distances relative to the well clear volume

$$\begin{aligned} h_{wc} &= h - wc_h \\ v_{wc} &= v - wc_v, \end{aligned} \quad (2)$$

h and v are the horizontal and vertical distances between the two aircraft, and wc_h and wc_v are the horizontal and vertical sizes of the well clear volume. It is noted that if a well clear violation occurs (the last option in (1)], the value is determined according to the dimension that has the worst incursion towards the NMAC volume. The severity of the incursion towards NMAC was evaluated as the ratio of the distance from the well clear boundary divided by the distance from the well clear and NMAC boundaries (the incursion would be 1.0 for an aircraft at the NMAC boundary). Thus, if the most severe incursion towards the NMAC volume is in the horizontal direction, then d_{wc} is reported as v_{wc}, and vise-versa.

Another fundamental metric is Closest Point of Approach (CPA)

$$CPA = \min\left(\sqrt{h^2 + v^2}\right). \quad (3)$$

Depending upon the type of encounter, one may be interested in CPA in either the horizontal or vertical directions

$$\begin{aligned} \text{CPA}_h &= \min\left(|h|\right) \\ \text{CPA}_v &= \min\left(|v|\right). \end{aligned} \quad (4)$$

CPA_h is useful, for instance, for horizontal (type) encounters wherein a vertical aircraft offset is used to enhance safety.

The distance to well clear metrics (d_{wc}, h_{wc}, and v_{wc}) can be drawn from a time different from that of CPA. Herein, distance to well clear metrics were recorded from the time of the most severe violation. Thus, if a vertical well clear violation occurred early within the OEP, the distance-to-well-clear metrics would differ significantly from CPA metrics, especially for horizontal distances. It is useful to track both, as CPA can occur at a time that does not correspond with a violation—even a well clear violation. One example of this is an intruder tracing a relative path where it passes over, but just well clear of ownship, while descending such that it crosses the well clear boundary at a horizontal separation greater than its vertical separation when it passed over ownship. In that case, CPA occurs when the intruder is above ownship, but a well clear violation occurs later and further away from ownship.

3.1.1.4 Summary and DAA Steps

The A18 test plan "Small UAS Detect and Avoid Requirements Necessary for Limited Beyond Visual Line of Sight (BVLOS) Operations: Separation Requirements and Testing: (Overarching) Test Plan" suggests providing data in the following tables:

- Summary
- Detect (D) Step
- Track (T) Step
- Evaluate (E) Step
- Maneuver (M) Step

Because the risk ratio is used to summarize DAA system performance, some have suggested that provision of information regarding different DAA steps is not needed. However, it is expected that some level of detail regarding the DAA steps will be desired by those who evaluate test results. This has been reinforced by discussions held within the ASTM WK62669 DAA Test Methods Task Group.

Summary and DAA Steps data are illustrated using results from flight tests. Summary data are provided in two tables. Table 9 contains summary data for entire encounters, while Table 10 contains data from the OEPs. For all of the tables except OEP tables, the first seven columns provide test execution characteristics. The rest of the columns contain test results. Speed data (CA, UA, and closure speeds) are not provided in the OEP tables, and thus test result data begin in column 6 of those tables.

The layout of entire encounter summary tables (e.g., Table 9) was altered relative to that used with the June 2020 tests. The need for coasting resulted in addition of a Coasted Flag (CFl) column. This flag indicates whether CPA, CPA_h, CPA_v, h_{wc}, v_{wc}, and d_{wc} metrics are from the non-coasted (0) or coasted (1) period. In addition, the Well Clear Violation (WCV) column was altered to provide values for the non-coasted period and the coasted period. CPA, CPA_h, and CPA_v were combined into one column, which created space for inclusion of uCPA, $uCPA_h$, and $uCPA_v$, the unmitigated CPA values discussed in the next section.

OEP tables are generated primarily to monitor aircraft altitude performance. The key metric is vertical aircraft separation. This is elucidated by providing information regarding aircraft altitudes, separations, and altitude variability in Table 10. Aircraft altitude characteristics are further discussed in Section 4.3.

Example DTEM tables are provided in Tables 11-14. As illustrated in these tables, DAA event characteristics that are captured are:

- Detect: First detection
- Track: First target information reception and track establishment
- Evaluate: Caution, warning, and maneuver identification
- Maneuver: Maneuver initiation and maneuver completion

DAA system characteristics that are captured are:

- Detect: Number of detections and False Target Rating (FTR)
- Track: Number of detections for track establishment

- Evaluate: Horizontal and vertical intruder location uncertainty at time of maneuver identification
- Maneuver: Maneuver type

The format of maneuver tables (e.g., Table 14) was altered to include a flag that indicates if the maneuver was completed during the coasted period (0=maneuver completed before coasted period, 1=maneuver completion during coasted period). Beyond this, the DTEM tables are as in Askelson (2022).

Some values in Tables 11-14 are missing. This results either because log files for these variables were not evaluated in the interest of time (number of detections in Table 11 and horizontal and vertical intruder location uncertainty at time of maneuver identification in Table 13) or because the DAA system did not produce these variables (cautions and warnings in Table 13) owing to the system not including an A&G function. It is noted that the “H/V Unc Mvr ID” field could be filled in with non-missing values. However, since ADS-B data were used, the values can be estimated from GPS performance characteristics (e.g., Table 8). It is also noted that “Dt from EB/H/V Mvr ID” is missing in Table 13 because the EO DCAPS Data Collector did not capture these events on 16 June 2021.

First detection values as shown in Table 11 and first target information reception and track establishment values as shown in Table 12 were produced by leveraging the fact that for the encounters the intruder was always within the detection and tracking range of the system. These values represent the first point at which the intruder would be detected after the beginning of the encounter, the time when first detection data would be communicated to the tracker after the beginning of an encounter (with an assumed delay of 0 s), and the time when a track would be established after the beginning of an encounter. These assume a worst-case 1 s offset between ADS-B data reception and the timing of GPS puck data. In the DAA system utilized herein, 3 detections are required for track establishment (Brian Murray 2021, personal communication).

Table 9. Summary data for 16 June 2021 encounters. Abbreviated titles are: B. Time=encounter Begin Time; E. Time=encounter End Time; Intr./UAS Spd=INTRuder Speed/UAS Speed; H/V Cls. Spd=Closure Speed in the Horizontal and Vertical directions; CFl=Coasted Flag (0 indicates CPA, CPA_h, CPA_v, h_{wc}, v_{wc}, and d_{wc} metrics from non-coasted period; 1 indicates these are from the coasted period); uCPA, $uCPA_h$, $UCPA_v$=unmitigated CPA, CPA_h, and CPA_v. Times are UTC (Universal Time Coordinated), speeds are in kts, Status indicates whether the encounter was acceptable (0=unacceptable, 1=acceptable); horizontal and vertical distances are in ft; and WCV (Well Clear Violation) indicates whether a well clear violation occurred and the type of violation (0=no violation, 1=well clear violation, 2=horizontal well clear violation, 3=vertical well clear violation), with the first value applying to the non-coasted period and the second value to the coasted period. Speeds, including horizontal and vertical closure speeds (H/V Cls. Spd) are averages from the period when both aircraft are inbound to the EFP. Large values consisting of the numeral '9' indicate missing values.

Scen. ID	Date	B. Time	E. Time	Intr./UAS Spd	H/V Cls. Spd	Status	CFl	CPA/ CPA_h/ CPA_v	uCPA/ $uCPA_h$/ $uCPA_v$	WCV	h_{wc}	v_{wc}	d_{wc}
HE-0-120	06/16/2021	1845:50	1847:38	96.10/ 39.24	56.95/ -0.52	1	1	3219.30/ 3182.97/ 482.28	99999999/ 36.88/ 9999999	0,0	1182.97	232.28	1205.55
HE-0-120	06/16/2021	1852:20	1854:00	97.86/ 66.57	164.32/ -1.48	1	1	6215.14/ 6201.37/ 413.39	99999999/ 2.87/ 9999999	0,0	4201.37	163.39	4204.55
HE-180-120	06/16/2021	1901:10	1903:00	102.65/ 37.90	64.80/ 1.25	1	1	3271.24/ 3249.03/ 380.58	99999999/ 29.56/ 9999999	0,0	1249.03	130.58	1255.84
HE-0-120	06/16/2021	1907:30	1908:40	9999999/ 999999	9999999/ 99999999	0							
HE-180-120	06/16/2021	1913:58	1915:00	84.44/ 37.85	45.50/ -3.28	1	1	3513.26/ 3485.23/ 442.91	99999999/ 50.37/ 9999999	0,0	1485.23	192.91	1497.71
HE-0-120	06/16/2021	1919:45	1920:43	91.60/ 71.63	163.57/ -2.46	1	1	6102.18/ 6082.04/ 495.41	99999999/ 21.72/ 9999999	0,0	4082.04	245.41	4089.41
HE-180-120	06/16/2021	1927:20	1928:13	91.29/ 42.28	49.42/ 4.92	1	1	3227.08/ 3195.62/ 449.48	99999999/ 1268.11/ 9999999	0,0	1195.62	199.48	1212.15

HE-0-120	06/16/2021	1933:05	1934:15	91.41/ 65.41	156.74/ -2.19	1	1	6386.08/ 6368.58/ 472.44	99999999/ 0.75/ 9999999	0,0	4368.58	222.44	4374.24

Table 10. OEP Summary data for 16 June 2021 encounters. Abbreviated titles are OEP BTime=OEP Beginning Time; OEP ETime=OEP End Time; Min h_{dist}=Minimum Horizontal DISTance between aircraft; UA Mean/Max-Mean/Mean-Min=UA MEAN height (AGL)/MAXimum height – MEAN height/MEAN height – MINimum height; CA Mean/Max-Mean/Mean-Min=MA MEAN height (AGL)/MAXimum height – MEAN height/MEAN height – MINimum height; Diff. Mean/Max/Min=MEAN/MAXimum/MINinum of aircraft height DIFFerences. Times, Status, and distance units are as in Table 9. Large values consisting of the numeral '9' indicate missing values.

Scen. ID	Date	OEP BTime	OEP ETime	Status	Min h_{dist}	UA Mean/Max-Mean/Mean-Min	CA Mean/Max-Mean/Mean-Min	Diff. Mean/Max/Min
HE-0-120	06/16/2021	1845:51	1847:38	1	3131.44	304.53/23.91/22.02	773.20/34.24/47.78	468.67/515.09/419.95
HE-0-120	06/16/2021	1852:55	1854:00	1	8031.97	330.97/23.71/35.34	778.41/29.03/26.74	447.44/475.72/406.82
HE-180-120	06/16/2021	1901:11	1903:00	1	3286.80	324.71/23.41/35.64	733.47/77.25/80.23	408.76/508.53/324.80
HE-0-120	9999999999	9999999	9999999	0				
HE-180-120	06/16/2021	1914:01	1915:00	1	3382.30	319.14/25.70/20.23	755.06/19.58/65.73	435.91/462.60/390.42
HE-0-120	06/16/2021	1919:46	1920:43	1	8560.08	320.35/17.93/24.72	764.62/46.10/45.76	444.27/498.69/387.14
HE-180-120	06/16/2021	1927:31	1928:13	1	3082.16	298.91/16.40/13.12	746.10/38.38/27.24	447.19/495.41/403.54
HE-0-120	06/16/2021	1933:06	1934:15	1	8446.04	309.69/25.31/17.34	766.01/44.71/34.03	456.32/498.69/400.26

Table 11. Detect (D) step data for 16 June 2021 encounters. Abbreviated titles are as in Table 9, with the additional abbreviations H/V Dist 1st Det=Horizontal/Vertical DISTances between aircraft at the time of 1st DETection; T1Det=Time of 1st DETection; # Det=Number of DETections during the encounter; FTR=False Target Rating [0=false targets not present, 1=false targets present but no factor, 2=false targets present and impacted system (e.g., delayed track establishment or track accuracy), 3=false targets prevented identification of actual target]. Times, Status, and distance units are as in Table 9. Large values consisting of the numeral '9' indicate missing values.

Scen. ID	Date	B. Time	E. Time	Intr./UAS Spd	H/V Cls. Spd	Status	H/V Dist 1st Det	T1Det	# Det	FTR
HE-0-120	06/16/2021	1845:50	1847:38	96.10/ 39.24	56.95/ -0.52	1	15164.70/ 442.91	1845:51	999999	1
HE-0-120	06/16/2021	1852:20	1854:00	97.86/ 66.57	164.32/ -1.48	1	24533.80/ 551.18	1852:21	999999	1
HE-180-120	06/16/2021	1901:10	1903:00	102.65/ 37.90	64.80/ 1.25	1	14526.29/ 439.63	1901:11	999999	1
HE-0-120	06/16/2021	1907:30	1908:40	9999999/ 999999	9999999/ 99999999	0				
HE-180-120	06/16/2021	1913:58	1915:00	84.44/ 37.85	45.50/ -3.28	1	9922.53/ 370.73	1913:59	999999	1
HE-0-120	06/16/2021	1919:45	1920:43	91.60/ 71.63	163.57/ -2.46	1	19681.91/ 410.11	1919:46	999999	1
HE-180-120	06/16/2021	1927:20	1928:13	91.29/ 42.28	49.42/ 4.92	1	8763.56/ 479.00	1927:21	999999	1
HE-0-120	06/16/2021	1933:05	1934:15	91.41/ 65.41	156.74/ -2.19	1	20841.58/ 439.63	1933:06	999999	1

Table 12. Track (T) step data for 16 June 2021 encounters. Abbreviated titles are as in Table 9, with the additional abbreviations Time/H/V Dist 1st TInfo=Time and Horizontal and Vertical DISTances between aircraft when 1st Target Information is received by the tracker; Time/H/V Dist Trk Establ=Time and Horizontal and Vertical DISTances between aircraft when a TRacK was ESTABLished; # Det=Number of DETections for track establishment. Times, Status, and distance units are as in Table 9. Large values consisting of the numeral '9' indicate missing values.

Scen. ID	Date	B. Time	E. Time	Intr./UAS Spd	H/V Cls. Spd	Status	Time/H/V Dist 1st TInfo	Time/H/V Dist Trk Establ	# Det
HE-0-120	06/16/2021	1845:50	1847:38	96.10/ 39.24	56.95/ -0.52	1	1845:51/ 15164.70/ 442.91	1845:54/ 14860.67/ 439.63	3
HE-0-120	06/16/2021	1852:20	1854:00	97.86/ 66.57	164.32/ -1.48	1	1852:21/ 24533.80/ 551.18	1852:24/ 24653.28/ 574.15	3
HE-180-120	06/16/2021	1901:10	1903:00	102.65/ 37.90	64.80/ 1.25	1	1901:11/ 14526.29/ 439.63	1901:14/ 14232.27/ 442.91	3
HE-0-120	06/16/2021	1907:30	1908:40	9999999/ 999999	9999999/ 99999999	0			
HE-180-120	06/16/2021	1913:58	1915:00	84.44/ 37.85	45.50/ -3.28	1	1913:59/ 9922.53/ 370.73	1914:02/ 9673.36/ 400.26	3
HE-0-120	06/16/2021	1919:45	1920:43	91.60/ 71.63	163.57/ -2.46	1	1919:46/ 19681.91/ 410.11	1919:49/ 18858.73/ 400.26	3
HE-180-120	06/16/2021	1927:20	1928:13	91.29/ 42.28	49.42/ 4.92	1	1927:21/ 8763.56/ 479.00	1927:24/ 8566.30/ 515.09	3
HE-0-120	06/16/2021	1933:05	1934:15	91.41/ 65.41	156.74/ -2.19	1	1933:06/ 20841.58/ 439.63	1933:09/ 20035.60/ 416.67	3

Table 13. Evaluate (E) step data for 16 June 2021 encounters. Abbreviated titles are as in Table 9, with the additional abbreviations Dt from EB/H/V Caution=Time difference (seconds) from Encounter Begin and Horizontal and Vertical aircraft separation at the time of CAUTION issuance; Dt from EB/H/V Warning=Time difference (seconds) from Encounter Begin and Horizontal and Vertical aircraft separation at the time of WARNING issuance; Dt from EB/H/V Mvr ID=Time difference (seconds) from Encounter Begin and Horizontal and Vertical aircraft separation at the time of ManeuVeR IDentification; H/V Unc Mvr ID=Uncertainty in intruder Horizontal and Vertical locations at the time of ManeuVeR IDentification. Times, Status, and distance units are as in Table 9. Large values consisting of the numeral '9' indicate missing values.

Scen. ID	Date	B. Time	E. Time	Intr./UAS Spd	H/V Cls. Spd	Status	Dt from EB/H/V Caution	Dt from EB/H/V Warning	Dt from EB/H/V Mvr ID	H/V Unc Mvr ID
HE-0-120	06/16/2021	1845:50	1847:38	96.10/ 39.24	56.95/ -0.52	1	999999/ 99999999/ 99999999	999999/ 99999999/ 99999999	999999/ 99999999/ 99999999	9999999/ 9999999
HE-0-120	06/16/2021	1852:20	1854:00	97.86/ 66.57	164.32/ -1.48	1	999999/ 99999999/ 99999999	999999/ 99999999/ 99999999	999999/ 99999999/ 99999999	9999999/ 9999999
HE-180-120	06/16/2021	1901:10	1903:00	102.65/ 37.90	64.80/ 1.25	1	999999/ 99999999/ 99999999	999999/ 99999999/ 99999999	999999/ 99999999/ 99999999	9999999/ 9999999
HE-0-120	06/16/2021	1907:30	1908:40	9999999/ 999999	9999999/ 99999999	0				
HE-180-120	06/16/2021	1913:58	1915:00	84.44/ 37.85	45.50/ -3.28	1	999999/ 99999999/ 99999999	999999/ 99999999/ 99999999	999999/ 99999999/ 99999999	9999999/ 9999999
HE-0-120	06/16/2021	1919:45	1920:43	91.60/ 71.63	163.57/ -2.46	1	999999/ 99999999/ 99999999	999999/ 99999999/ 99999999	999999/ 99999999/ 99999999	9999999/ 9999999
HE-180-120	06/16/2021	1927:20	1928:13	91.29/ 42.28	49.42/ 4.92	1	999999/ 99999999/ 99999999	999999/ 99999999/ 99999999	999999/ 99999999/ 99999999	9999999/ 9999999
HE-0-120	06/16/2021	1933:05	1934:15	91.41/ 65.41	156.74/ -2.19	1	999999/ 99999999/ 99999999	999999/ 99999999/ 99999999	999999/ 99999999/ 99999999	9999999/ 9999999

Table 14. Maneuver (M) step data for 16 June 2021 encounters. Abbreviated titles are as in Table 9, with the additional abbreviations Time/H/V Dist Mvr Init=Time and Horizontal and Vertical aircraft separation/DISTances at the time of ManeuVeR INITiation; Mvr Cmp Cst Fl=ManeuVeR CoMPletion during CoaST period Flag (0=maneuver completed before coast period, 1=maneuver completed during coast period); Time/H/V Dist Mvr Comp=Time and Horizontal and Vertical aircraft separation/DISTances at the time of ManeuVeR COMPletion; Mvr Type=ManeuVeR TYPE (‘L’=left turn, ‘R’=right turn, ‘C’=climb, ‘D’=descend). Times, Status, and distance units are as in Table 9. Large values consisting of the numeral ‘9’ indicate missing values.

Scen. ID	Date	B. Time	E. Time	Intr./UAS Spd	H/V Cls. Spd	Status	Time/H/V Dist Mvr Init	Mvr Cmp Cst Fl	Time/H/V Dist Mvr Comp	Mvr Type
HE-0-120	06/16/2021	1845:50	1847:38	96.10/ 39.24	56.95/ -0.52	1	1847:03/ 8249.27/ 485.56	1	1847:40/ 3186.23/ 482.28	R
HE-0-120	06/16/2021	1852:20	1854:00	97.86/ 66.57	164.32/ -1.48	1	1853:20/ 15014.33/ 475.72	1	1854:30/ 6204.89/ 413.39	L
HE-180-120	06/16/2021	1901:10	1903:00	102.65/ 37.90	64.80/ 1.25	1	1902:07/ 8409.76/ 367.45	1	1902:47/ 3250.02/ 380.58	R
HE-0-120	06/16/2021	1907:30	1908:40	9999999/ 999999	9999999/ 99999999	0				
HE-180-120	06/16/2021	1913:58	1915:00	84.44/ 37.85	45.50/ -3.28	1	1914:18/ 8443.35/ 446.19	1	1915:04/ 3490.88/ 442.91	R
HE-0-120	06/16/2021	1919:45	1920:43	91.60/ 71.63	163.57/ -2.46	1	1920:03/ 14995.10/ 446.19	1	1921:23/ 6083.16/ 495.41	L
HE-180-120	06/16/2021	1927:20	1928:13	91.29/ 42.28	49.42/ 4.92	1	1927:34/ 7758.50/ 485.56	1	1928:14/ 3198.02/ 449.48	R
HE-0-120	06/16/2021	1933:05	1934:15	91.41/ 65.41	156.74/ -2.19	1	1933:28/ 15026.69/ 492.13	1	1934:57/ 6371.60/ 472.44	L

3.1.1.5 Separation Timeline

The fundamental metrics associated with DAA commonly reduce to separation and timing. A means for illustrating these was developed and labelled as a separation timeline, which is a plot of aircraft separation as a function of time. The time variable utilized herein is seconds prior to unmitigated CPA, which would occur if neither aircraft maneuvered and continued to fly the heading and speed utilized during their inbound segment. Because aircraft headings and speeds varied during the inbound segments, the smallest ("best case") unmitigated CPA was utilized. For horizontal encounters, unmitigated CPA_h and horizontal separations are utilized. For encounters that include closure in the vertical direction, CPA and total separation are utilized.

Development of the relations required for these computations is provided by Askelson (2022) and is not repeated here. The reader is referred to Askelson (2022) for details.

3.1.2 Campaign Metrics

3.1.2.1 (Sample) Risk Ratio

The loss of well clear risk ratio *LR* is given by

$$LR = \frac{\sum_{i=1}^{N} I_i n_i LR_i}{\sum_{i=1}^{N} I_i n_i}, \tag{5}$$

where LR_i is the loss of well clear risk ratio for the ith encounter geometry, n_i is the number of encounters for the ith geometry, and I_i is a weighting factor that allows one to apply more weight to certain encounter geometries than others. The latter might be utilized, for instance, if certain geometries are determined to be more likely (or important) than other geometries. Herein, I_i=1. It is noted that one could give certain geometries more weight than others by executing more encounters (greater n_i) for those geometries.

Because data for a subset of horizontal and vertical collision geometries are considered, sample *LR* values herein are labelled with the symbol $LR_{\subseteq c}$, given by

$$LR_{\subseteq c} = \frac{\sum_{i=1}^{N} I_i n_i LR_{c\_i}}{\sum_{i=1}^{N} I_i n_i}, \tag{6}$$

where LR_{c_i} is the loss of well clear sample risk ratio for the ith 'collision' (horizontal or vertical) geometry.

3.1.2.2 Sample Risk Ratio Uncertainty

Understanding uncertainties associated with *LR* is important, as they provide context regarding the potential range of values and whether values are consistent with other estimation methods (e.g., simulation). Multiple approaches to estimating uncertainty have been investigated by Askelson (2022). These approaches are used herein. The reader is referred to Askelson (2022) for details.

3.2 Software/Processing

3.2.1 Language

Because of the need to produce results quickly and because of its rich, publicly-available software set, Python 3 (Van Rossum and Drake 2009) was used. It is noted that numerous software modules, including visualization and a module for performing great circle calculations, were utilized.

3.2.2 Organization

Two sets of software were developed—software for processing individual encounters and software for producing overall campaign results. For convenience, the encounter processing occurs for each flight test day. Thus, the software sets are referred to as 'ByDay' and 'Campaign'.

3.2.2.1 ByDay Software

The processing flow is:

- Obtain/set program control variables
- Check program invocation
- Obtain DCAPS data
    - Delineates encounters
    - Provides additional information such as when the EO identified the maneuver
- Obtain aircraft position data (GPS puck data)
- Obtain ADS-B data for the (if requested)
- Compute encounter events, statistics, and characteristics
    - Determine when aircraft are inbound
    - Identify encounter events and compute distance metrics
        - Loss/regain of well clear, horizontal well clear, and vertical well clear
        - Aircraft horizontal and vertical separation as a function of time
        - CPA, CPA_h, and CPA_v
    - Identify the OEP
    - Compute additional distance metrics and refine encounter events
        - d_{wc}, h_{wc}, and v_{wc}
        - Refine vertical well clear data using OEP
        - Determine times of loss/regain of well clear, horizontal well clear, and vertical well clear
    - Compute metrics that are relevant when both aircraft are inbound
        - Determine when both aircraft are inbound
        - Compute average speeds for each aircraft when both are inbound
        - Compute closure speeds (horizontal and vertical) while both aircraft are inbound
    - Compute height statistics
        - Aircraft maximum and minimum heights during encounters
        - Aircraft maximum, minimum, and mean heights during the OEP
    - Compute minimum horizontal aircraft separation during the OEP
- Compute DTEM statistics
    - Compute Detect statistics
    - Compute Track statistics
    - Compute Evaluate statistics

- Compute Maneuver statistics
- Compute coasted tracks for UA (if requested)
- Compute separation timeline statistics
  - Compute unmitigated CPA or CPA_h
  - Compute aircraft distances and times prior to unmitigated CPA from when both aircraft are inbound to the end of the OEP
  - Compute aircraft distances and times prior to unmitigated CPA for encounter descriptors (e.g., when both aircraft are inbound) and DTEM DAA event characteristics (first detection, maneuver initiation, etc.).
- Output summary results to files
  - Output to text files
  - Output to Microsoft® Word® compatible files
- Output DTEM results to files
  - Output to text files
  - Output to Microsoft® Word® compatible files
- Create "XY" plots (described in results section
- Create box plots (described in results section
- Create overview plots (described in results section)
- Create separation timeline plots

Changes to the 'ByDay' code base include significant and minor changes. Significant changes include alterations to the primary executable file that enables use of the code with different field campaigns (including setting constants associated with those campaigns) and computation of coasted UA paths. The latter required, in addition to computation of coasted paths, computation of distance metrics (e.g., CPA) and events (e.g., well clear violation) during the coasted period and alterations to plotting and file output software to illustrate/provide-output-regarding the coasted period.

3.2.2.2 Campaign Software

The processing flow is:

- Set program control variables
- Check program invocation
- Ingest encounter summary (overview and OEP) data (produced using ByDay software)
- Organize the summary data according to encounter type, horizontal intruder test speed, vertical encounter angle, and horizontal encounter angle.
- Compute statistics
  - Compute maximum, minimum, mean, median, and standard deviation of CPA_h value groups (encounter type, horizontal intruder test speed, vertical encounter angle, and horizontal encounter angle)
  - Compute $LR_{\subseteq c}$ for user-specified groups (user indicates how data are grouped—e.g., a user can indicate that all HEs and DEs at a specified horizontal intruder test speed can be grouped)
  - Test distribution of CPA_h values in user-specified groups for normality
  - Determine which distribution best fits CPA_h values in user-specified groups
  - Estimate $LR_{\subseteq c}$ uncertainty using the non-homogeneous method

    - Estimate $LR_{\subseteq c}$ uncertainty using the homogeneous binomial proportion confidence interval
    - Estimate $LR_{\subseteq c}$ uncertainty using the Normal distribution method
- Output results (statistical CPA_h information) for encounter sets
- Create plots
    - Plot encounter events
    - Create distance vs. sets plots (described in results section)
    - Create density function plots
        - Cumulative Density Function (CDF; from data)
        - Theoretical CDF (from statistical properties of data)
        - Best and worst-case CDFs and associated values at the well-clear boundary [second homogeneous uncertainty estimation method (Askelson 2022)]
        - Theoretical Probability Density Function (PDF; from statistical properties of data)

Inclusion of DEs drove a significant rewrite of the Campaign software. This rewrite enables organization of results (e.g., CPA_h) into groups. For instance, all results conducted with a set horizontal intruder speed (e.g., 120 kts) can be grouped for estimation of *LR*. The analyst controls what encounter test characteristics belong to a group. Thus, this approach provides significant flexibility when analyzing test data like those considered herein.

An additional modification relative to Askelson (2022) is, for some calculations, inclusion of encounter data only if an encounter could produce the relevant violation. This follows the definition of *LR* risk ratio in that an encounter should be considered only if a violation was possible with that encounter. Data from an HE are used to compute statistical results (e.g., $LR_{\subseteq c}$ and $LR_{\subseteq c}$ uncertainty) only if unmitigated $CPA_h \leq 2000$ ft [the horizontal well-clear distance used in ASTM (2020)]. Moreover, data from a DE are used to compute statistical results only if unmitigated $CPA_h \leq 2000$ ft and unmitigated $CPA_v \leq 250$ ft [the vertical well-clear distance used in ASTM (2020)]. These criteria for DEs are strict given that well clear status was being maintained through horizontal maneuvers. It is noted that September 2020 test data were re-processed using these criteria with no appreciable effect on results for that test campaign.

4 TEST RESULTS

4.1 Flight Summary

A summary of encounters executed during the test campaign is provided in Tables 15 and 16. As indicated in Table 15, 50 encounters were desired. This resulted from 10 tests for each of 4 different HEs/horizontal encounter angles and 5 tests for each of 2 different DEs/horizontal encounter angles. The goal of 50 was missed by one encounter owing to a determination after the testing period that one of the HE-225-120 encounters was unacceptable. In Table 15, the note regarding UA performance resulted from the excellent wind tolerance of the aircraft, which significantly helped the team collect the required data in the allotted time period, and the speed of the UA that enabled maintenance of well clear.

Table 16 delineates June 2021 flight test encounters by scenario. As indicated in Table 16, the goal for number of acceptable tests were missed by one for scenarios HE_180_120 and HE_225_120, with one extra test executed for HE_0_120.

Table 15. Summary of June 2021 flight test encounters by day.

Day	Number of Acceptable Encounters	Comments
Monday	0	Shakedown/technical challenges with ownship.
Tuesday	0	Technical challenges with ownship resolved late in day.
Wednesday	7	Enhanced ownship reporting.
Thursday	24	Several unacceptable rerun; aircraft has amazing performance.
Friday	18	1 unacceptable rerun
Total	49	50 desired

Table 16. Summary of June 2021 flight test encounters by scenario.

Encounter	Number of Desired Encounters	Number of Acceptable Encounters
HE_0_120	10	11
HE_45_120	10	10
HE_180_120	10	9
HE_225_120	10	9
DE_0_2_120	5	5
DE_135_2_120	5	5
Total	50	49

4.2 Encounter Events

Figure 16 provides a summary of encounter events—loss/retention of horizontal, vertical, and overall well clear status—for both the non-coasted and coasted periods. As indicated in Figure 16, no well clear or horizontal well clear events occurred during the non-coasted or coasted periods. This underscores UA performance, which was effectively flown away from conflict owing in large part to its relatively high cruise speeds (up to ~66 kts). Given the results in Figure 16, it is apparent that $LR_{\subseteq c}$ = 0.0 for this test campaign.

The five vertical well clear violations forecasted to occur during the coasted periods of encounters occurred only with DEs and result from the approach used to coast flight paths. For the CA, coasted altitudes differ from the end altitude from the period used to compute coasting characteristics if that period is dominated by ascent or descent (70% or more of the period is characterized by ascent or descent). For the UA, coasted altitudes differ from the end altitude from the period used to compute coasting characteristics if 50% or more of that period is characterized by non-zero vertical speeds. For the June 2021 tests, the CA threshold of 70% was reached 5 times and the UA threshold of 50% was not reached. An example of a forecasted vertical well-clear violation is provided in Figure 17. As indicated in Figure 17, user-specified minimum altitude limits are used when producing coasted altitudes (herein, 500 ft AGL for the CA and 50 ft AGL for the UA).

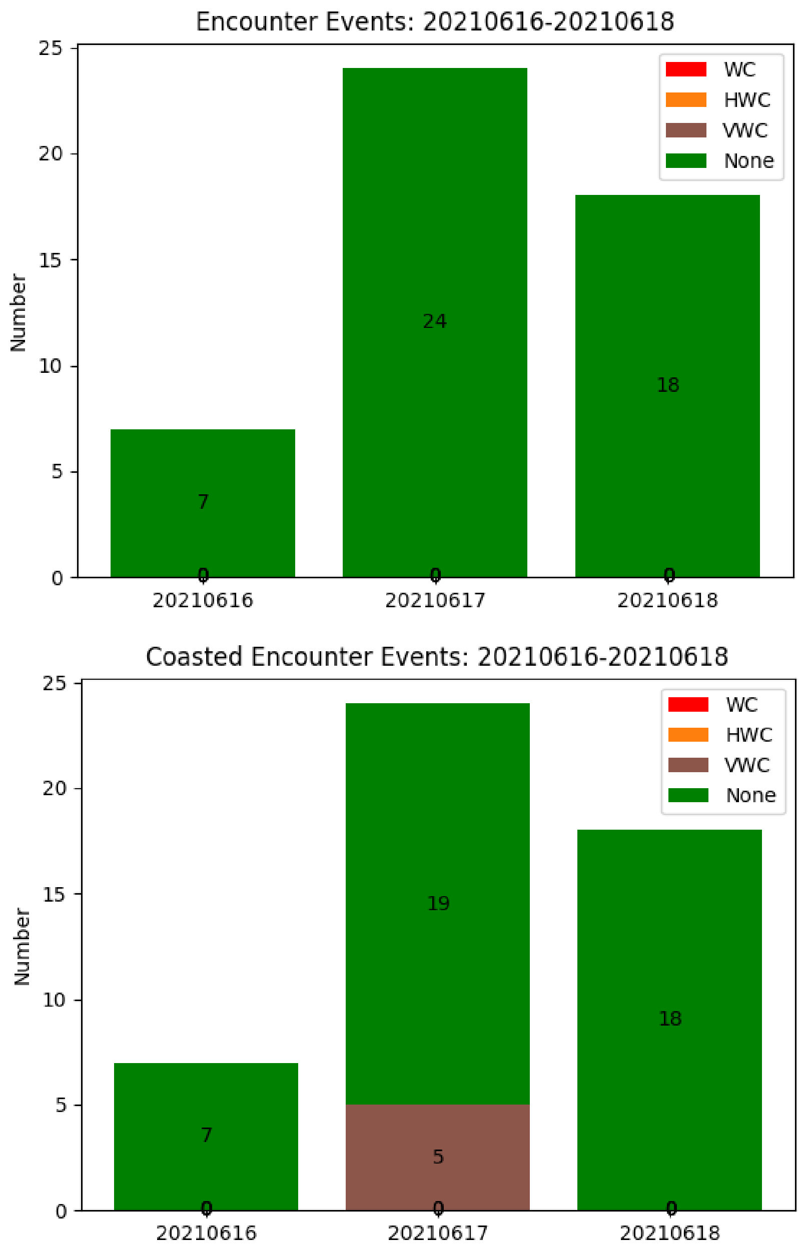

Figure 16. Encounter events for the June 2021 flight test encounters. The top image is for the non-coasted period and the bottom image is for the coasted period.

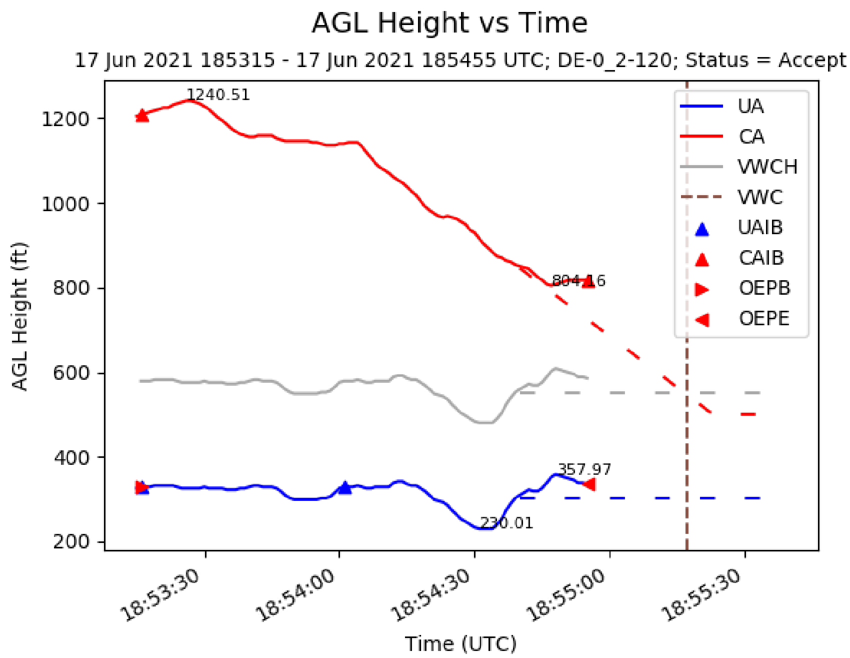

Figure 17. Illustration of a forecasted coasted-period vertical well clear violation. Plot parameters are UA AGL altitudes (relative to the EFP altitude) in blue, CA AGL altitudes in red, AGL altitudes during the coasted period indicated by long-dashed lines, the CA altitudes needed to maintain vertical well clear in dark grey, the times of vertical well clear violation indicated by dashed bown lines (well clear and horizontal well clear are indicated by dashed red and orange lines, respectively), the UA inbound portion indicated by blue triangles, the CA inbound portion indicated by red triangles, and the OEP beginning and end indicated by rotated red triangles.

4.3 Vertical Separation Integrity

OEP altitude performance is considered herein. Extrapolated altitudes from coasted periods are not considered, as challenges with extrapolation could produce confusing results regarding altitude performance.

As in Askelson (2022), for HEs variability of UA altitudes was generally smaller than that for CA altitudes. However, CA altitude variability approached that associated with the UA, which was not common in Askelson (2022) (e.g., Figure 18). As in Askelson (2022), CA altitudes were generally, but not always, within ±50 ft of mean OEP altitude.

Use of a larger vertical safety offset (400 ft vs. 350 ft) did enable maintenance of vertical well clear. The primary enabler, however, was CA altitude monitoring. During tests, if CA altitude was deemed to be too low, personnel from the Electronic Observer Trailer requested that the CA increase its altitude. The impact of this is apparent in Figure 18, with CA altitudes being notably higher after the first encounter, after which such a request was made. It is noted that mean CA altitude was also too low during the first few encounters on 17 June 2021. This resulted in the minimum vertical aircraft separation during the campaign of 252 ft occurring during the first encounter on 17 June 2021 (not shown). The approach wherein a vertical safety offset was maintained by halting CA descent during DEs worked well, with a minimum OEP vertical aircraft offset during the 10 DEs of 403 ft.

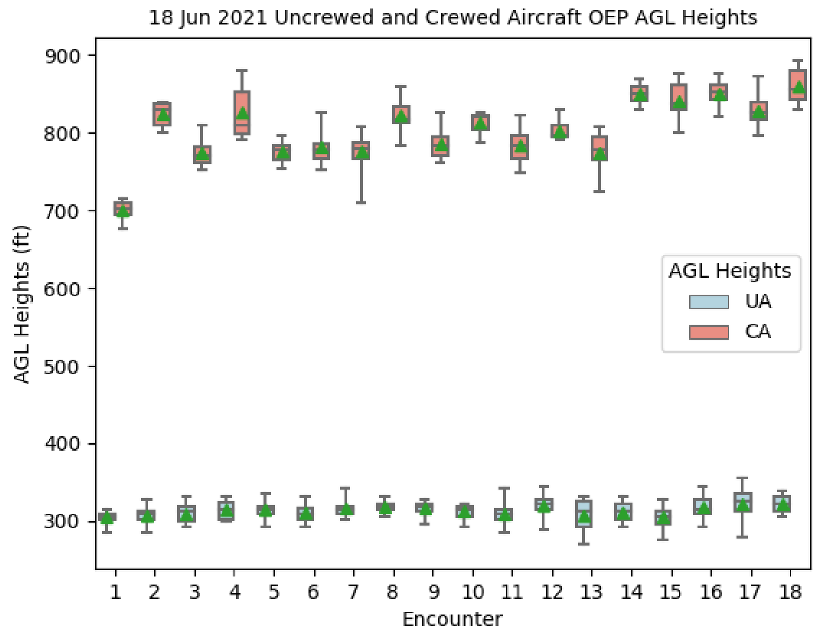

Figure 18. Box-and-whisker plot of 18 June 2021 aircraft AGL altitudes. Box edges indicate the lower and upper quartiles, the lines within the boxes indicate medians, the green triangles indicate means, and the whiskers encapsulate the full ranges of values.

4.4 Example Encounters

An example DE is illustrated in Figure 19. The separation timeline in this figure illustrates a challenge that was encountered with the DE_135_2_120—timing. For some reason, none of the DE_135_2_120 encounters were timed such that unmitigated $CPA_h \leq 2000$ ft and unmitigated $CPA_v \leq 250$ ft. Thus, none of these encounters were used in computation of some statistical quantities, such as $LR_{\subseteq c}$ and $LR_{\subseteq c}$ uncertainty. In this instance, the timing failure is indicated by the values of unmitigated CPA_h and CPA_v (red plus symbols in the separation timeline) in Figure 19. It is also indicated by CPA occurring prior to the coasted period. This was relatively uncommon, occurring 0 times on 16 June 2021, 4 times on 17 June 2021 (all DEs), and 1 time on 18 June 2021 (HE). Another interesting aspect of the encounter illustrated in Figure 19 is the increased horizontal closure rate that occurred after maneuver initiation, which is indicated by the more rapid decrease in horizontal separation with time. Askelson (2022) noted this phenomenon for encounters that have a significant overtaking component. Examination of separation timelines for the June 2021 test campaign (not shown) indicates that such an increase in closure rate commonly occurs for encounters that have a significant overtaking component.

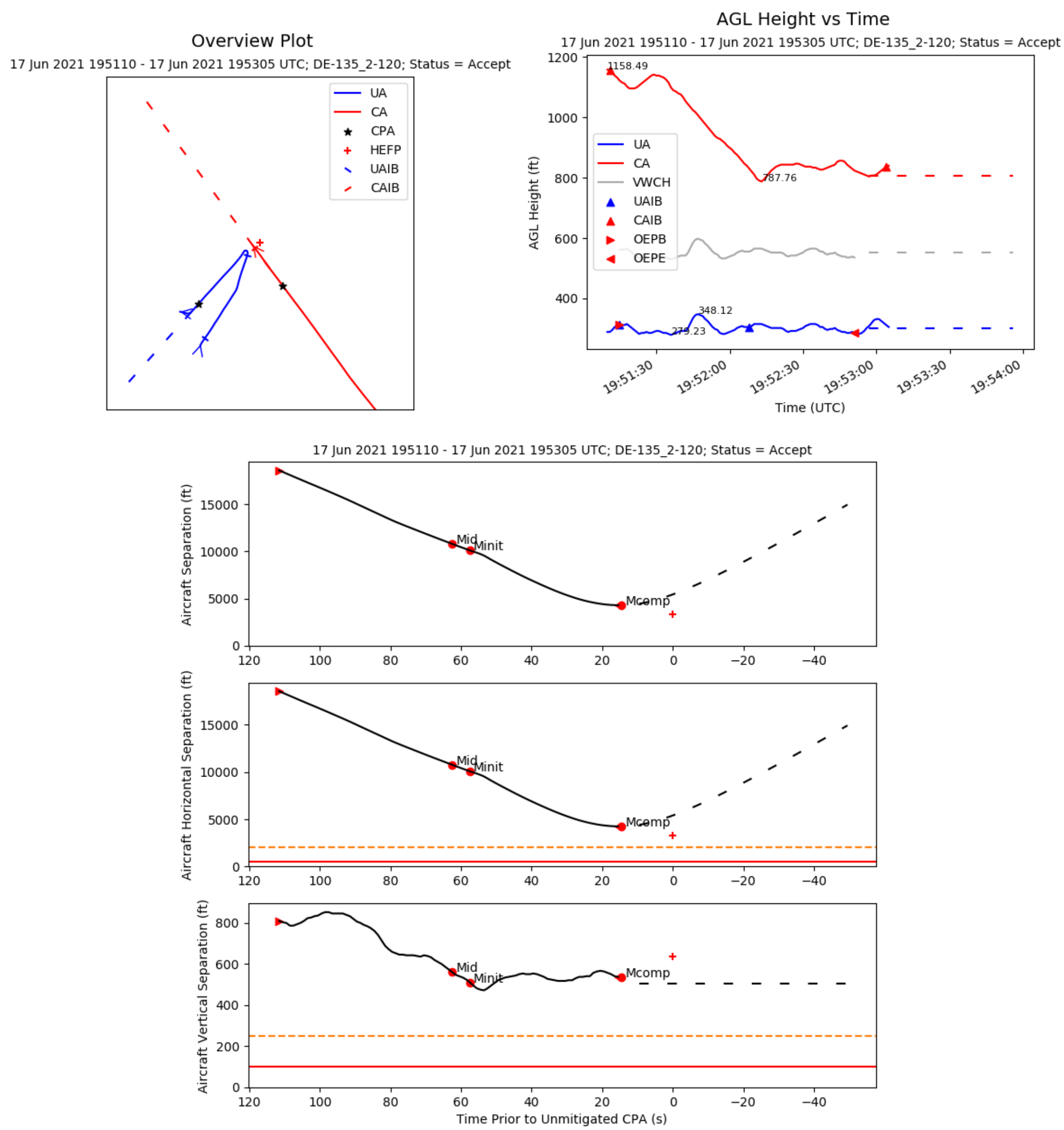

Figure 19. Illustration of the 155110-195305 UTC 17 June 2021 encounter. Upper left provides a plan view, with the UA flight path in blue, CA flight path in red, CPA indicated with a black star symbol, the EFP indicated with a red plus symbol, the inbound portions of flight indicated by blue (UA) and red (CA) dashes perpendicular to the flight paths, and the dashed lines indicating the coasted period. Upper right is as in Figure 17. Bottom is the separation timeline (top to bottom is total, horizontal, and vertical separation), with the solid black lines indicating the non-coasted period and dashed black lines indicating the coasted period; the well clear boundaries indicated by the orange dashed lines; the NMAC boundaries indicated by the solid red line; unmitigated CPA, CPA_h,, and CPA_v indicated by the red plus symbols; the time when both aircraft are inbound indicated with rotated red triangles (left sides of plots); the OEP end indicated with rotated red triangles (right sides of plots); and labels indicating the following: Dfst=First Detection, Testblsh = Track Establishment, Ecaut = Caution, Ewarn = Warning, Mid = Maneuver Identification, Minit = Maneuver Initiation, and Mcomp = Maneuver Completion.

4.5 Impact of Collecting more Samples for Encounter Scenarios

One of the objectives of this test campaign is evaluation of the impact of collecting more samples for encounter scenarios. To explore this, results from the 100 kt intruder speed tests conducted during the September 2020 campaign (Table 17) and the tests (120 kt intruder speed tests) conducted during the June 2021 campaign (Table 18) are compared. In Tables 17 and 18, the standard deviation of the mean μ is given by

$$\sigma_\mu = \frac{\sigma}{\sqrt{N}}, \tag{7}$$

which is the relation for the large-sample limit with σ the population standard deviation and N the number of samples. Herein, the sample standard deviation is used as an estimate for σ. The relation (7) generally applies when $N \geq 30$ regardless of the underlying distribution of the random variable owing to the central limit theorem (e.g., Mendenhall et al. 1990, §7.3). This relation is used herein in the absence of a general estimator for small samples sizes.

The standard deviation of the standard deviation is estimated using

$$\sigma_\sigma = s\frac{\Gamma\left(\frac{N-1}{2}\right)}{\Gamma\left(\frac{N}{2}\right)}\sqrt{\frac{N-1}{2}-\left[\frac{\Gamma\left(\frac{N}{2}\right)}{\Gamma\left(\frac{N-1}{2}\right)}\right]^2}, \tag{8}$$

where s is the sample standard deviation and Γ is the gamma function. This relation applies for normal distributions (Lehman and Casella 1998, p. 92), and is approximated as

$$\sigma_\sigma = \frac{s}{\sqrt{2(N-1)}}, \tag{9}$$

which holds for $N > 10$ (Ahn and Fessler 2003). While CPA_h values are not necessarily normally distributed, this relation is used in the absence of a more general formulation. Given the limitations of (7) and (8), both are considered to provide approximations, and not exact values, for σ_μ and σ_σ.

For the HEs and common horizontal encounter angles in Tables 17 and 18 (0°, 45°, 180°, and 225°), standard deviations of CPA_h are not always smaller with a larger number of samples (nearly equal for 0°, smaller for June 2021 tests for 45° and 180°, and larger for June 2021 tests for 225°). As a percentage of standard deviation s, however, σ_μ and σ_σ were smaller for the June 2021 tests (Tables 19 and 20). Doubling the number of tests for a scenario roughly decreased the percentage of s of σ_μ and σ_σ by 10%. These decreases are consistent with (7) and (9) since, with s inserted for σ in (7),

$$\frac{\sigma_\mu}{s} = \frac{1}{\sqrt{N}}, \tag{10}$$

and

$$\frac{\sigma_\sigma}{s} = \frac{1}{\sqrt{2(N-1)}}. \tag{11}$$

For $N = 5$, (10) and (11) produce 0.45 and 0.35, while for $N = 10$, (10) and (11) produce 0.32 and 0.24. These are consistent with the results in Tables 19 and 20.

Table 17. Scenario-based encounter characteristics for September 2020 tests conducted with 100 kt intruder speed. Num Encs = NUMber of ENCounterS; Num HWCV = Number of Horizonal Well-Clear Violations; LR is the loss of well clear sample risk ratio for a set of encounters; Maximum is the maximum CPA_h; Minimum is the minimum CPA_h; Mean is the average CPA_h; Median is the median CPA_h; Std Dev is the STanDard DEViaton of the CPA_h values; Std Dev Mean is the STanDard DEViation of the Mean for the set of CPA_h values; Kurtosis is the statistical parameter that indicates “tailedness” of the set of CPA_h values; and Std Dev Std Dev is the STanDard DEViation of the STanDard Deviation for the set of CPA_h values. Units for variables that have units are ft. Only encounters that satisfy the unmitigated well clear criteria are considered.

Scen. ID	Num Encs	Num HWCV	LR	Maximum	Minimum	Mean	Median	Std Dev	Std Dev Mean	Kurtosis	Std Dev Std Dev
HE_0_0_100	5	0	0.000	5938.30	3154.96	4600.78	4905.12	1246.83	557.60	1.32	452.60
HE_45_0_100	6	0	0.000	6160.14	3510.73	4940.85	4910.39	962.39	392.89	1.91	311.06
HE_90_0_100	4	1	0.250	6310.70	1759.60	3820.09	3605.03	1921.26	960.63	1.85	810.80
HE_135_0_100	6	1	0.167	6010.33	1588.01	4364.95	4493.63	1537.29	627.59	2.93	496.87
HE_180_0_100	4	2	0.500	2698.34	433.78	1604.24	1642.42	1140.85	570.42	1.11	481.46
HE_225_0_100	5	2	0.400	2819.22	1518.95	2080.22	2226.45	535.83	239.63	1.73	194.51
HE_270_0_100	4	1	0.250	4212.76	1266.08	3289.00	3838.59	1390.89	695.44	2.16	586.98
HE_315_0_100	4	3	0.750	4316.22	976.88	2177.47	1708.38	1473.05	736.52	2.19	621.65

Table 18. As in Table 17 but for June 2021 tests conducted with 120 kt intruder speed.

Scen. ID	Num Encs	Num HWCV	LR	Maximum	Minimum	Mean	Median	Std Dev	Std Dev Mean	Kurtosis	Std Dev Std Dev
HE_0_0_120	11	0	0.000	6970.64	3182.97	5329.59	5622.52	1214.88	366.30	2.06	274.86
HE_45_0_120	9	0	0.000	8328.86	5994.67	7448.76	7706.65	700.12	233.37	3.10	177.57
HE_180_0_120	7	0	0.000	3761.21	2797.08	3335.09	3249.03	348.31	131.65	1.93	102.44
HE_225_0_120	9	0	0.000	8263.48	4508.53	6341.09	5943.95	1178.00	392.67	2.08	298.77
DE_0_2_120	4	0	0.000	4479.52	3928.82	4193.73	4183.30	282.52	141.26	1.08	119.23

Table 19. Scenario-based relative magnitudes (to standard deviation *s*) of standard deviation of the mean σ_μ and standard deviation of the standard deviation σ_σ for September 2020 tests conducted with 100 kt intruder speed. Labels are as described in Table 17 and in the main text.

Scen. ID	Num Encs	s	σ_μ	σ_σ	$100(\sigma_\mu/s)$	$100(\sigma_\sigma/s)$
HE_0_0_100	5	1246.83	557.60	452.60	44.72	36.30
HE_45_0_100	6	962.39	392.89	311.06	40.82	32.32
HE_180_0_100	4	1140.85	570.42	481.46	50.00	42.20
HE_225_0_100	5	535.83	239.63	194.51	44.72	36.30

Table 20. As in Table 19 but for June 2021 tests conducted with 120 kt intruder speed.

Scen. ID	Num Encs	s	σ_μ	σ_σ	$100(\sigma_\mu/s)$	$100(\sigma_\sigma/s)$
HE_0_0_120	11	1214.88	366.30	274.86	30.15	22.62
HE_45_0_120	9	700.12	233.37	177.57	33.33	25.36
HE_180_0_120	7	348.31	131.65	102.44	37.80	29.41
HE_225_0_120	9	1178.00	392.67	298.77	33.33	25.36

4.6 Sample Risk Ratio and Sample Risk Ratio Uncertainty

The value of $LR_{\subseteq c}$ for the June 2021 test campaign is provided in Figure 20. As indicated earlier, no horizontal well clear violations occurred and, thus, $LR_{\subseteq c}$ = 0.0. The uncertainty window for $LR_{\subseteq c}$ is very small, being 0.0-0.01 for the inhomogeneous method described by Askelson (2022). Both homogeneous methods produced uncertainty windows of 0.0-0.02. The box and whisker plot shown in Figure 20 indicates that CPA_h characteristics may be inhomogeneous, as indicated in Askelson (2022), with the HE_180_0_120 encounter set having significantly lower values.

Figure 20 also highlights that some encounters did not satisfy unmitigated well clear criteria (unmitigated $CPA_h \leq 2000$ ft for HEs and unmitigated $CPA_h \leq 2000$ ft and unmitigated $CPA_v \leq$ 250 ft for DEs). This is illustrated in Table 21. As that table shows, 1 HE_45_120, 2 HE_180_120, 1 DE_0_2_120, and all 5 DE_135_2_120 encounters did not satisfy these criteria. The loss of 9 encounters resulted in 40 being used to estimate $LR_{\subseteq c}$ and $LR_{\subseteq c}$ uncertainty. In future tests, a means for modifying intruder speed during the inbound phase should be utilized to ensure that each encounter satisfies unmitigated well clear criteria.

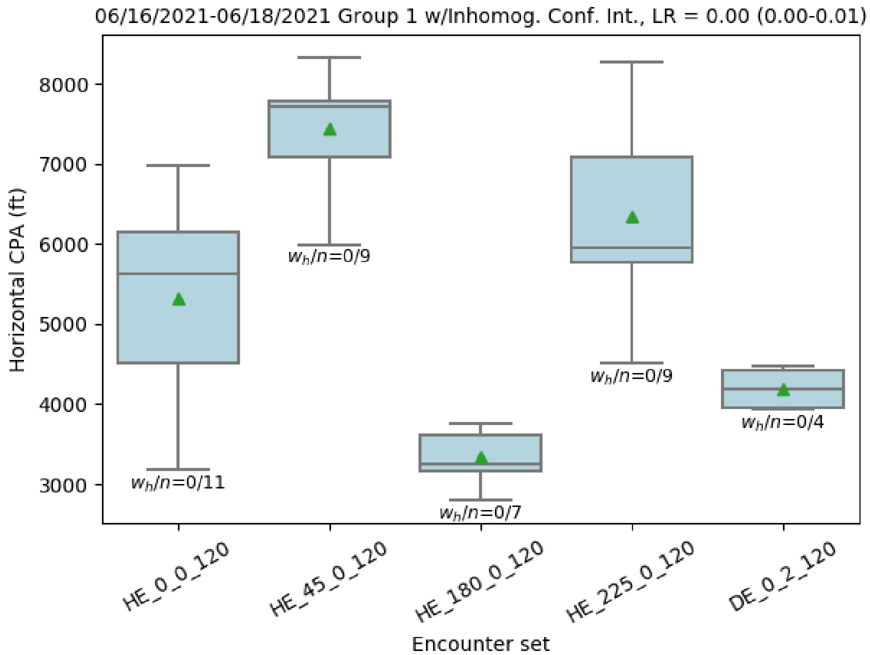

Figure 20. Box and whisker plots of CPA$_h$ for the June 2021 test campaign. Box and whisker features are as in Figure 18. The symbol w_n indicates the number of horizontal well clear violations (including well clear violations) and the symbol n indicates the total number of encounters for each encounter geometry. $LR_{\subseteq c}$ values are provided in the figure title, with the corresponding uncertainty window in parentheses.

Table 21. Summary of encounters that did not satisfy the unmitigated well clear criteria.

Encounter	Number of Acceptable Encounters	Number of Encounters Satisfying Unmitigated Well Clear Criteria
HE_0_120	11	11
HE_45_120	10	9
HE_180_120	9	7
HE_225_120	9	9
DE_0_2_120	5	4
DE_135_2_120	5	0
Total	49	40

Results for the second homogeneous approach (assuming a Normal distribution) described by Askelson (2022) are illustrated in Figure 21. As shown in this figure, the Cumulative Density Function (CDF) of the data does not perfectly conform to a Normal distribution shape. This could occur because the underlying distribution is not normal or because of chance (a result of obtaining a finite sample of values). It is also noted that the uncertainty window does not correspond with the numbers that are superimposed on the plotted distributions. This occurs because the plotted distributions are shifted relative to the actual data. To avoid confusion relative to the calculated $LR_{\subseteq c}$ value (from the data), differences between the theoretical and best- and worst-case CDFs are used to determine the size of the uncertainty window, which is centered on the computed $LR_{\subseteq c}$ value.

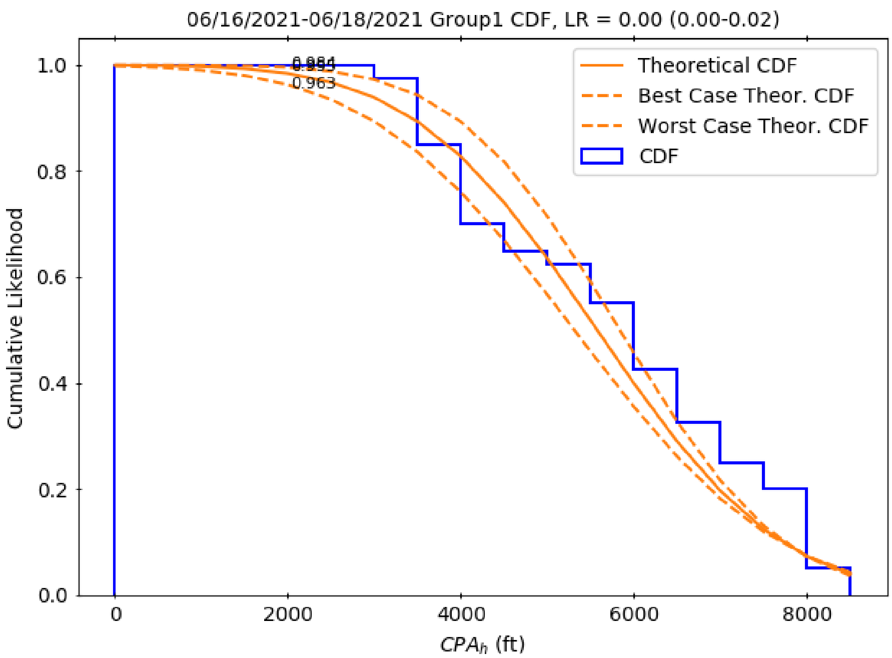

Figure 21. CDFs of CPA_h for the June 2021 test campaign. The solid blue line indicates the CDF directly from the data, the solid orange line indicates the CDF derived from statistical properties of the data (mean and standard deviation), the dashed orange lines are the best- and worst-case CDFs (top and bottom, respectively), and numbers indicate the likelihood $CPA_h \geq 2000$ ft for the respective distribution.

5 CONCLUSIONS

5.1 Lessons Learned

Lessons learned from this round of flight tests include:

- Failures associated with testing occur, including ones experienced during this round of flight tests:
    - Ingestion of UA telemetry into the DAA system can be a major challenge. It resulted in a significant delay in data collection during the June 2021 tests.
- Detection challenges occur
    - ADS-B drop-outs did occur and seemed to be focused on a certain location.
    - Primary tracks (radar) did not always arise for aircraft taking-off and landing at the airport.
- Display glitches can occur

- Occasionally the locations of UA and CA did not update on RangeVue™ Pro
  - This resulted in aircraft positions “jumping”.

5.2 Utilization in ASTM WK62669 DAA Test Methods Task Group

The results from this round of testing are being utilized in the ASTM WK62669 DAA Test Methods Task Group. Topics that are being leveraged include:

- Flight test approach (geometric)
- Data elements/metrics

This group has identified use of a model as a means for demonstrating compliance with requirements. This approach requires that the model be validated, with flight testing being part of that validation. Results from Askelson (2022) and the June 2021 tests have been leveraged to identify metrics that can be utilized for model validation. These metrics are designed to be, to the extent possible, independent of each other, which simplifies estimation of probabilities/likelihoods should such estimation be useful. The current recommended set of metrics includes:

- Aircraft separation (e.g., h for horizontal encounter) or Time Prior To Reference Time (TPTRT) at the time of first detection.
- Time after first detection when the track is established.
- Time from track establishment to maneuver initiation.
- Δd from time of maneuver initiation to CPA (e.g., in horizontal direction for horizontal-type encounters).
- Maneuver type

In this list, TPTRT is relative to a user-chosen reference time. This list is likely to change—addition of metrics for alerts that are part of ASTM (2020), for example. They provide a foundation, however, and are based upon Askelson (2022) and this effort. It is noted that based upon the subsequent discussion, other metrics may be used in place of CPA. Furthermore, the first 4 metrics in this list are quantitative, while the last is qualitative and indicates what kind of maneuver was executed (e.g., turn right, descend and turn left, etc.).

Concepts associated with the d_{wc} metric have been leveraged to provide a recommendation to this group regarding fundamental distance metrics that should be used when comparing simulation and test results. For tests like those described herein and in Askelson (2022), horizontal maneuvers are utilized to maintain (horizontal) well clear status. Thus, the fundamental metric is minimum horizontal aircraft separation h_{min}. If vertical maneuvers are used to maintain (vertical) well clear status (presumably with a horizontal offset for safety), then the fundamental metric would be minimum vertical aircraft separation v_{min}. It is noted that quantities obtained using CPA do not necessarily correspond to h_{min} or v_{min}. For example, when horizontal maneuvers are utilized to maintain (horizontal) well clear, CPA_h may not equal h_{min} owing to concurrent changes in vertical separation. Given that horizontal closure rates should generally overwhelm changes in vertical aircraft separation, non-correspondence between these two metrics should be rare. This was evaluated for the September 2021 tests and only one instance where the time of CPA_h and of h_{min} were different was identified. In that instance, the times differed by 1 s and CPA_h and h_{min} differed by 1.21 ft. It is noted that the d_{wc} metric also captures values at the time of minimum horizontal or vertical separation under specified conditions (horizontal or vertical well clear violation).

The impact of the d_{wc} metric upon recommendations regarding fundamental distance metrics is most pronounced in the situation where maneuvers in both directions are utilized to maintain well clear status. This situation has been discussed in this working group, with an initial recommendation, if one value is to be reported, of determining the direction in which the incursion is worse. In this case, worse is defined by the dimension that incorporates the greatest background risk. This is determined using Weinert et al. (2018), from which the well clear recommendation of wc_h = 2000 ft and wc_v = 250 ft is an expression of background risk.[5] Given that de facto expression of constant risk, similar shapes (having the same shape but different sizes) are considered to also be expressions of risk that is roughly constant on a given surface/shape. It is important to recognize that the NMAC volume, which has dimensions of 500 ft horizontally and 100 ft vertically, is also a de facto expression of risk. Thus, between the well clear boundary and the NMAC boundary a 10 ft horizontal increment (2000 ft – 500 ft = 1500 ft) corresponds to a 1 ft vertical increment (250 ft – 100 ft = 150 ft) in terms of risk. In the recommendation presented to the working group, h_{min} or v_{min} is reported depending upon which is proportionately closer to the NMAC boundary, with horizontal distance to the NMAC boundary divided by 10 for comparison with vertical distance to the NMAC boundary. This concept of worst incursion is the same as that used with d_{wc} for well clear violations.

The distance metric recommendation for the case of maneuvering in both the horizontal and vertical directions is flawed because one could have a very small separation in either direction while the separation in the other direction is large. When that happens, the recommendation indicates relatively high risk when, in fact, risk was low. This issue is illustrated in Figure 22. The UA-relative CA trajectory in Figure 22 applies when both aircraft are moving, but for simplicity one can consider the UA in Figure 22 to be stationary (hovering) while the CA is flown along the illustrated path. With the recommendation that was provided to the test methods group, point A would be the point for which v_{min} is reported (assuming the aircraft are co-altitude when the CA is at the time of A). However, from a risk perspective, a time around the time of point B is the relevant time because risk is maximized around that time. To properly capture this, the time of maximum risk $t_{mr}(i_{mr})$ can be determined using

$$i_{mr} = \arg\min\left\{ \max\left(\frac{h_1}{wc_h}, \frac{v_1}{wc_v}\right), \max\left(\frac{h_2}{wc_h}, \frac{v_2}{wc_v}\right) \ldots, \max\left(\frac{h_n}{wc_h}, \frac{v_n}{wc_v}\right) \right\}, \tag{12}$$

where i_{mr} is the index when risk is maximized [the index for the set of encounter times when the values in the brackets in (12) is smallest] and n is the total number of times for which aircraft separation is computed. Division by wc_h and wc_v in (12) normalizes the h and v distances by the sizes of the well clear boundary. For each time for which aircraft separation is computed, saving the maximum of h/wc_h and v/wc_v retains the normalized risk surface for that time. Obtaining the minimum then provides the index/time when risk was maximized (the normalized risk surface was smallest). Both horizontal and vertical distances at the time of maximum risk, h_{mr} and v_{mr}, can be utilized when comparing with simulations. Alternatively, the h_{mr} or v_{mr} that identifies the risk surface, which is the horizontal or vertical value depending upon which has the higher normalized (relative to wc_h and wc_v) distance, can be used for comparison with simulations.

[5] Constant risk surfaces, which express the unmitigated (e.g., no aircraft maneuvers owing to identification of the other aircraft) risk of NMAC given encounters between a UA and CA, do not conform exactly to a hockey-puck shape. However, given the adaptation of that shape, it and similar shapes (having the same shape but different sizes) are a de facto expression of constant risk.

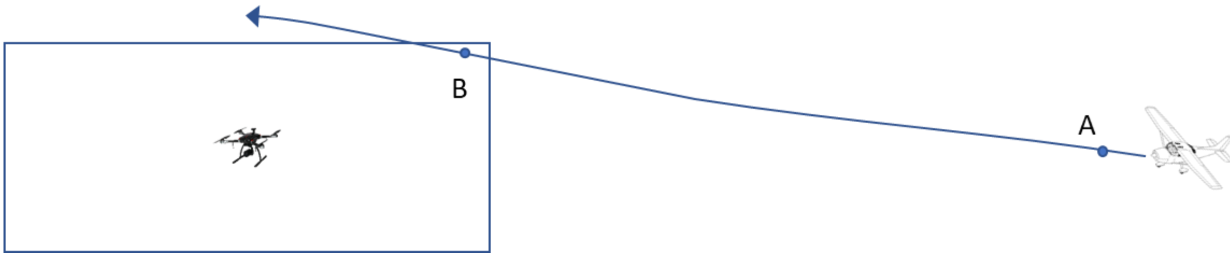

Figure 22. Illustration of the challenge with identifying the point of highest risk during an encounter. The box around the UA represents the well clear boundary, the line emanating from the CA represents the UA-relative CA trajectory, and A and B are points discussed in the main text. Features are not drawn to scale.

5.3 Future Work

Numerous topics should be evaluated further. These include:

- Inclusion of other variations in flight tests (curved trajectories, climb-into encounters, etc.).
- Ensuring safety while including other variations in flight tests.
- Environmental impacts—especially impacts of the wind on the ability to maintain well clear status. It is expected that a UA maneuver into the wind will increase the risk ratio and decrease CPA values.
- Definition of what agreement/correspondence between simulation and flight test results is.
- Identification of more general relations (do not assume a Normal distribution) for the standard deviation of both mean values and standard deviation values—especially for small sample sizes.

5.4 Summary

A summary of the test plan for this test event is provided. This includes:

- Background Information: Standards efforts and encounter characteristics
- Objectives
- Personnel
- DAA system
- Aircraft
- Test locations
- Test dates and schedule
- Test conditions
- Test cards
- Data collection and management

This test plan follows Askelson (2022) and leverages a geometric approach to gathering data, in which potential encounter geometries are varied. While it does not include evaluation of speed variations, it does include descend-into encounters.

The vertical aircraft safety offset was increased 50 ft relative to that used by Askelson (2022) to 400 ft. This helped ensure desired aircraft separation. The biggest enabler for ensuring maintenance of vertical well clear during testing, however, was CA altitude monitoring in which CA altitudes were adjusted if they were deemed to be too low. These resulted in no vertical well clear violations occurring during the June 2021 test campaign.

As subset of horizontal encounter geometries (0°, 45°, 180°, 225°) were tested for horizontal encounters and two horizontal encounter geometries (0°, 135°) and one vertical encounter geometry (2°) were tested for descend-into encounters. The descend-into vertical encounter geometry is consistent with a typical general aviation aircraft descent rate of 500 ft min^{-1}. To evaluate the impact of executing more tests for a given scenario, 10 encounters were planned for each horizontal encounter scenario. For each of the descend-into scenarios, five encounters were planned. For 3 of the 6 scenarios, the desired number of tests was not achieved (1 more for the 0° horizontal encounter scenario and 1 less for the 180° and 225° horizontal encounter scenarios).

For descend-into encounters, CA descent was halted to preserve a 400 ft vertical safety offset between aircraft. The pilots were very successful at halting their descent as planned, as the minimum vertical offset for the 10 descend-into encounters was 403 ft.

It is noted that use of a DAA system that utilized ADS-B data (and a ground-based radar data) resulted in the challenge of maintaining well-clear being focused on the EM steps of DTEM. Disregarding data drop-outs, maintaining well clear was driven by evaluating and maneuvering early enough in the encounters. Such a system has very limited detection range dependency, which results in less sensitivity to closure rates/intruder speeds.

The metrics used generally followed those of Askelson (2022). Some changes were needed, however. These include addition of a coast period, which is needed because of flight of the UA under Part 107 rules, without the use of daisy-chained observers, and the speed of the UA resulting in it reaching the visual range limit associated with Part 107 prior to the time when aircraft separation was minimized. When that limit was reached, the aircraft was directed to station-keep (fly circles around a defined location). To obtain results consistent with a BVLOS type of operation in which such station-keeping would not generally occur, the straight-line portion of the UA path associated with its maneuver was extrapolated forward/coasted.

Software previously developed by Askelson (2022) was updated in numerous ways. One important update is evaluation of whether a violation relevant for that type of encounter would occur if the UA did not maneuver. This follows the definition of loss of well clear risk ratio in that an encounter should be considered only if a violation was possible with that encounter. Data from an HE are used to compute statistical results (e.g., LR and LR uncertainty) only if unmitigated $CPA_h \leq 2000$ ft [the horizontal well-clear distance used in ASTM (2020)]. Moreover, data from a DE are used to compute statistical results only if unmitigated $CPA_h \leq 2000$ ft and unmitigated $CPA_v \leq 250$ ft [the vertical well-clear distance used in ASTM (2020)]. Ten encounters did not satisfy these requirements, which resulted from improper timing of the inbound aircraft segments. None of the descend-into encounters having a horizontal encounter angle of 135° satisfied the requirement of an unmitigated well clear violation. The causes of significant timing issues for that encounter scenario are unknown. In future tests, a means for modifying intruder speed during the inbound phase should be utilized to ensure that each encounter satisfies unmitigated well clear criteria.

No horizontal well clear violations occurred during this test campaign, resulting in a loss of well clear risk ratio for this subset of encounter scenarios of $LR_{\subseteq c} = 0.0$. $LR_{\subseteq c}$ uncertainty windows for the inhomogeneous and two homogeneous approaches described by Askelson (2022) are 0.0-0.01 and 0.0-0.02, respectively. The exceptional performance of the SuperVolo UA that was used in these tests—especially its cruising speed (up to ~66 kts), significantly enabled maintenance of horizontal well clear. This is consistent with Kaabouch et al. (2020), who showed that UA speed can significantly reduce the likelihood of a well clear violation.

Execution of more encounters for given scenarios did not consistently reduce the standard deviation of CPA_h (aircraft separation) values. It did, however, reduce uncertainty in both the mean and standard deviation of CPA_h values. The value of this relative to the additional cost associated with executing more encounters is unknown.

These results must be placed in context with the broader set of possible encounters, the breadth of which can be evaluated through simulation. Moreover, the metrics utilized herein for the major stages of DAA, which were developed through the need for information regarding how the system is performing and qualified by pragmatic considerations (e.g., timing challenges associated with data collection), provide useful information regarding these major stages (and are being considered by the ASTM WK62669 DAA Test Methods Task Group). Finally, encounter summary test metrics different from CPA_h utilized herein that are consistent with background risk—h_{min} and v_{min}—are suggested for future characterization and comparison with simulations.

Bibliography

Ahn, S., and J. A. Fessler, 2003: Standard Errors of Mean, Variance, and Standard Deviation Estimators. 2 pp., https://web.eecs.umich.edu/~fessler/papers/files/tr/stderr.pdf.

Askelson, M. A., 2022: Small UAS Detect and Avoid Requirements Necessary for Limited Beyond Visual Line of Sight (BVLOS) Operations: Task 6 UND September 2020 Flight Test Report. USDOT FAA (ASSURE), 84 pp.

Askelson, et al., 2017: Small UAS Detect and Avoid Requirements Necessary for Limited Beyond Visual Line of Sight (BVLOS) Operations. USDOT FAA (ASSURE), 516 pp.

ASTM 2020: Standard Specification for Detect and Avoid System Performance Requirements. F3442/F3442-20, 22 pp.

C Speed, 2021: Lightwave Radar. Accessed 12 April 2021, http://www.cspeed.com/radar.

Deaton, J. L., and R. J. Hansman, 2019: Investigating Collision Avoidance for Small UAS Using Cooperative Surveillance and ACAS X. ICAT-2019-06. 126 pp.

e-CFR, 2021a: Part 135— Operating Requirements: Commuter and on Demand Operations and Rules Governing Persons on Board Such Aircraft. Accessed 15 September 2021, https://www.ecfr.gov/current/title-14/chapter-I/subchapter-G/part-135?toc=1.

e-CFR, 2021b: Part 107—Small Unmanned Aircraft Systems. Accessed 21 April 2021, https://www.ecfr.gov/cgi-bin/text-idx?node=pt14.2.107&rgn=div5.

Edwards, M. W., M. J. Kochenderfer, J. K. Kuchar, and L. P. Espindle, 2009: Encounter Models for Unconventional Aircraft Version 1.0. Project Report ATC-348, 84 pp.

FAA William J. Hughes Technical Center, 2021: Wide Area Augmentation System Performance Analysis Report—October 2021. Report #78, 200 pp., https://www.nstb.tc.faa.gov/reports/2021_Q3_FAA_WAAS_PAN_Report_78_v1.0.pdf.

Griffith, J. D., M. W. M. Edwards, R. M. C. Miraflor, and A. J. Weinert, 2013: Due Regard Encounter Model Version 1.0. Project Report ATC-397, 56 pp.

ICAO, 2014: Aeronautical Communications: Volume IV—Surveillance and Collision Avoidance Systems (Annex 10 to the Convention on International Civil Aviation). 216 pp.

Kaabouch, N., M. Mullins, K. Foerster, and M. Askelson, 2020: Small UAS Detect and Avoid Requirements Necessary for Limited Beyond Visual Line of Sight (BVLOS) Operations: Separation Framework Report. USDOT FAA (ASSURE), 58 pp.

L3Harris, 2019: RANGVUE™: Beyond Visual Line of Sight Situational Awareness for UAS, 2 pp., https://www.l3harris.com/sites/default/files/2020-07/as_mn_datasheet_rangevue.pdf.

L3Harris, 2021: ADS-B Xtend™ for Airports. Accessed 12 April 2021, https://www.l3harris.com/all-capabilities/ads-b-xtend-airports.

Lehman, E. L., and G. Casella, 1998: *Theory of Point Estimation*. 2nd Ed., Springer, 589 pp.

Mendenhall, W., D. D. Wackerly, and R. L. Scheaffer, 1990: *Mathematical Statistics with Applications*. 4th Ed., PWS-Kent, 818 pp.

Qstarz, 2021: BT-Q1000XT. Accessed 6 June 2021, http://www.qstarz.com/Products/GPS%20Products/BT-Q1000XT-F.htm.

RTCA, 2017: Minimum Operational Performance Standards (MOPS) for Detect and Avoid (DAA) Systems. RTCA, Inc., 838 pp.

Schäfer, M., M. Strohmeier, V. Lenders, I. Martinovic, and M. Wilhelm, 2014: Bringing up OpenSky: A large-scale ADS-B sensor network for research. *IPSN-14 Proc. 13th Int. Symp. on Inf. Proc. in Sensor Networks*, 83-94.

Stones Mobile Radio, 2021: Stonecast. Accessed 19 April 2021, https://www.stonesmobileradio.com/products/stonecast-tower-network/.

Underhill, N. K., E. P. Harkleroad, R. E. Guendel, A. J. Weinert, D. E. Maki, and M. W. M. Edwards, 2018: Correlated Encounter Model for Cooperative Aircraft in the National Airspace System Version 2.0. Project Report ATC-440, 138 pp.

USDOT, 2021: Satellite Navigation – Wide Area Augmentation System (WAAS). Accessed 6 June 2021. https://www.faa.gov/about/office_org/headquarters_offices/ato/service_units/techops/navservices/gnss/waas.

Van Rossum, G., and F. L. Drake, 2009: *Python 3 Reference Manual*. Scotts Valley, CA., 242 pp.

Weinert, A., and G. Barrera, 2020: A review of low altitude manned aviation operations. Preprints 2020, 2020070522, doi: 10.20944/preprints202007.0522.v1, https://www.preprints.org/manuscript/202007.0522/v1.

Weinert, A. J., E. P. Harkleroad, J. D. Griffith, M. W. Edwards, and M. J. Kochenderfer, 2013: Uncorrelated Encounter Model of the National Airspace System Version 2.0. Project Report ATC-404, 93 pp.

Weinert, A, S. Campbell, A. Vela, D. Schuldt, and J. Kurucar, 2018: Well-clear recommendation for small unmanned aircraft systems based on unmitigated collision risk. *J. Air Transp.*, **26**, 113-122.

Weinert, A., N. Underhill, and A. Wicks, 2019: Developing a low altitude manned encounter model using ADS-B observations. *IEEE Aerospace Conference 2019*, Big Sky, MT, https://ieeexplore.ieee.org/document/8741848.

Appendix A: High-Level Overview of Test Process

Tests are based upon test scenarios, which are labelled according to encounter geometry and intruder speed. The encounter scenarios are indicated using the following nomenclature:

- HE_45_120: Horizontal Encounter at a 45° horizontal encounter angle and for a 120 kt intruder (at a 0° vertical encounter angle).
- CE_45_-2_120: Climb-into Encounter (CE) at a 45° horizontal encounter angle and -2° vertical encounter angle for a 120 kt intruder.
- DE_45_2_120: Descend-into Encounter at a 45° horizontal encounter angle and 2° vertical encounter angle for a 120 kt intruder.

Test roles include:

- Flight test director: The person who is responsible for overall coordination of encounters, including declaration of checkpoints.
- Uncrewed Aircraft (UA) PIC: Person responsible for operation of the UA.
- Crewed Aircraft (CA; intruder) pilot: Person responsible for operation of the CA/intruder.
- Visual Observer (VO): Assists UA PIC with see and avoid function.
- Data collector: A person who helps collect data (e.g., records times of events).
- Electronic Observer: Monitors a display system that provides a visualization of the test range, including real-time locations of ownship, intruder, and the Encounter Focal Point (EFP).
- Tech support: Keeps technology functioning during test. This maybe a combination of industry support and ASSURE A18 performers.

Test Waypoints are:

- EFP: The location at which both aircraft would arrive at the same time if a safety offset (horizontal or vertical) or maneuver was not employed.

Test Checkpoints are:

- Uncrewed aircraft Setup Exit (USE): The time at which the UA exits its orbit to proceed to scenario start.
- Scenario Start (SS): This is declared by the flight test director once the time for arrival at the EFP for both aircraft is within tolerance.
- Encounter Initiation (EI): The time at which the flight test director declares that the encounter has begun (based upon criteria provided below). A data collector records this.
- First Detection (FD): The time at which the DAA system first detects the intruder. A data collector records this.
- Track Establishment (TE): The time at which a track for the intruder is established. This is recorded either automatically using software or by a data collector.
- Maneuver Initiation (MI): The time of ownship maneuver initiation. This is recorded either automatically using software or by a data collector.
- Encounter End (EE): The time at which the flight test director declares that the encounter has ended. A data collector records this. After this, both aircraft move to set up (S) the next encounter.

The testing process for a horizontal encounter is illustrated in Figure A1. The sequence of events is described in the HE test cards for a horizontal encounter angle of 0°.

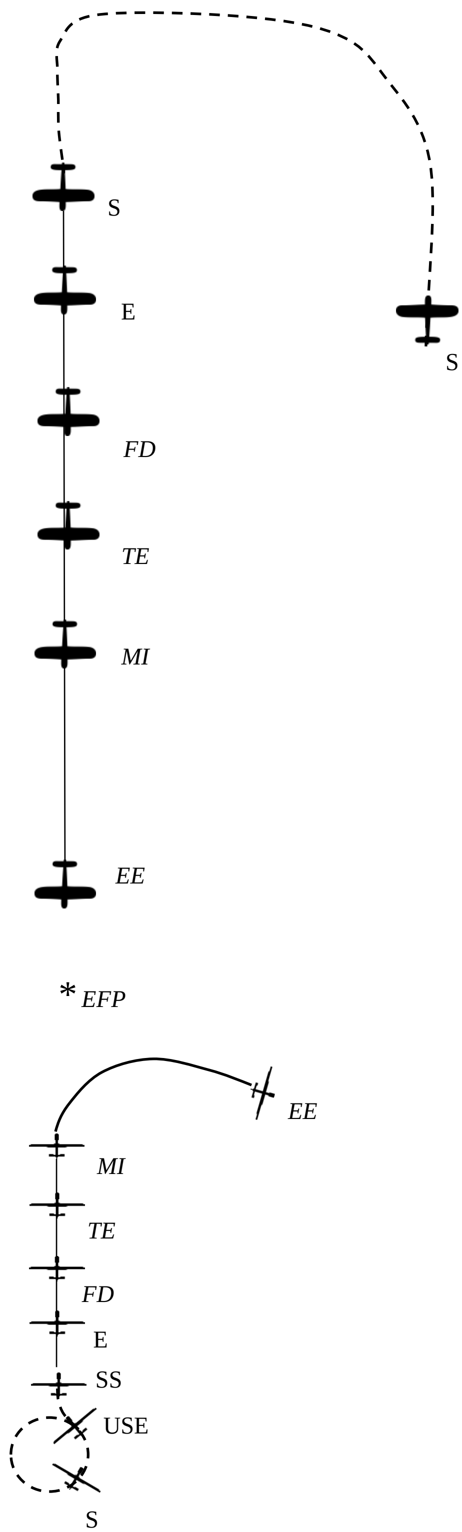

Figure A1. Illustration for an HE test with horizontal encounter angle of 0°.

Appendix B: Test Cards/Scripts for UND/NPUASTS 13-19 June 2021 Tests

A total of 18 cards [(4 HE scenarios + 2 DE scenarios) x 1 intruder speed x 3 roles] support this test campaign. For clarity, different cards are used for the roles of flight test director (Master/overall), the intruder, and the UAS. Example test cards for DE_0_2_120 are provided in the following pages; the full set of scripts/cards is not provided for brevity.

Overall Test Card

Flight Card #	A18-ND-MASTER-DE-0_2-120	
Date/Time		
Objective		
Description	Manned aircraft and UAS encounters are conducted at the indicated cruise speeds. The manned aircraft starts at 1100 feet AGL and descends down to 800 feet AGL at 500 feet/min. A vertical offset of 400' used to provide safety margin.	
UAS Platform	Supervolo	
UAS Altitude	390 ft	
UAS Speed	40 knots	
Intruder	Piper Archer	
Intruder Altitude	1100 - 800 ft	

1

The FAA's Center of Excellence for UAS Research ASSURE Alliance for System Safety of UAS through Research Excellence

The FAA's UAS Center of Excellence for UAS Research ASSURE Alliance for System Safety of UAS through Research Excellence

NORTHERN PLAINS UAS TEST SITE

Intruder Speed	120 knots
Location	47.328505, -97.087696. Lovas Farmstead.
GCS	Mission Planner
DAA System ID	L3Harris GBDAA
DAA Sensors	Xtend ADS-B Receiver, C-Speed Radar, FAA NextGen (VAS)
Supporting Technology	NPUASTS trailers, visualization systems, additional ADS-B receivers, video cameras, DCAPS data recording
Intruder Pilot	
RPIC	
VOs	
MC	
FD	
COA/Waiver(s)	

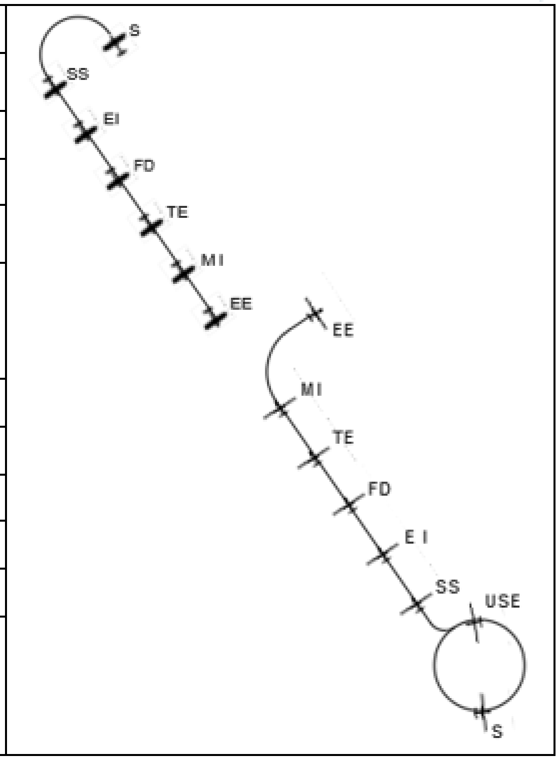

Condition # (objective)					
✓		Action	Remarks	Call	Time
	1a	UA maintains position at defined stand-off location ~5649 ft (~1.07 mi) from the Horizontal Encounter Focal Point (HEFP) as manned aircraft flies loop away from encounter location to set-up (S) for this encounter.	Point E 47.315149°, -97.075449°	RPIC calls "holding at point E"	
	1b	Intruder executes turn at defined ground point ~17,160 ft (~3.25 mi) from HEFP during (S) at 1100 feet AGL.	This is driven by the DAA technology, the warning/alert system, and UA speed. 47.365509°, -97.126405°	Intruder calls "Holding NW"	
	1c	Intruder begins flying straight along its encounter path towards Scenario Start (SS).			
	1d	UA exits (S) and proceeds towards SS once intruder begins exits its set-up turn.		Flight test director calls UA set up exit (USE).	

2

	1e	Intruder varies speed to ensure arrival at HEFP within tolerance.			
	1f	Altitudes are checked through radio calls.			
	2	Arrival time at the HEFP is within tolerance—Scenario Start (SS) is declared.	Difference between arrival times at HEFP is ≤ 6.5 s.	Flight test director calls SS.	
	2a	Intruder aircraft begins descending at 500 feet per minute down to 800 feet AGL.		Flight test director calls "begin descent"	
	3	Encounter Initiation (EI) is declared.	Occurs after SS and no later than approximate time of first alert or warning.	Flight test director calls EI.	
	4a	Time of First Detection (FD) is recorded.	Data collector records the time of FD. If FD does not occur, this is noted.		
	4b	Time of Track Establishment (TE) is recorded.	Data collector records the time of TE. If TE does not occur, this is noted.		
	4c	Time of Maneuver Initiation (MI) is recorded.	Data collector records the time of MI. If MI does not occur, this is noted.	RPIC calls "maneuvering"	
	4d	Approximate time of CPA is recorded.	If a maneuver occurs, data collector records approximate time of CPA. Exact time is determined with post-processing.		
	4e	Well clear status recorded.	If known, data collector records status (maintained or not).		
	4f	Regain well-clear time recorded	If well clear is not maintained, data collector records approximate time it is regained. Exact time is determined with post-processing..		
	5	Encounter End (EE) is declared.	Data collector records the time of encounter end (same as scenario end).	Flight test director declares EE.	
	6	Both aircraft proceed to set-up (S) for next encounter (if applicable).			

3

UA Test Card

Flight Card #	A18-ND-UA-DE-0_2-120	
Date/Time		
Objective		
Description	Manned aircraft and UAS encounters are conducted at the indicated cruise speeds. The manned aircraft starts at 1100 feet AGL and descends down to 800 feet AGL at 500 feet/min. A vertical offset of 400' used to provide safety margin.	
UAS Platform	Supervolo	
UAS Altitude	390 ft	
UAS Speed	40 knots	
Intruder	Piper Archer	
Intruder Altitude	1100 - 800 ft	

1

Intruder Speed	120 knots
Location	47.328505, -97.087696. Lovas Farmstead.
GCS	Mission Planner
DAA System ID	L3Harris GBDAA
DAA Sensors	Xtend ADS-B Receiver, C-Speed Radar, FAA NextGen (VAS)
Supporting Technology	NPUASTS trailers, visualization systems, additional ADS-B receivers, video cameras, DCAPS data recording
Intruder Pilot	
RPIC	
VOs	
MC	
FD	
COA/Waiver(s)	

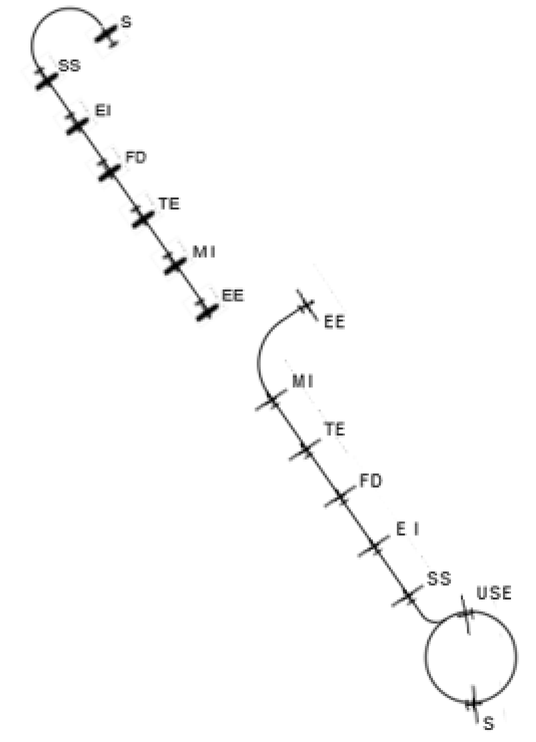

Condition # (objective)					
✓		Action	Remarks	Call	Time
	1a	UA maintains position at defined stand-off location ~5649 ft (~1.07 mi) from the Horizontal Encounter Focal Point (HEFP) as manned aircraft flies loop away from encounter location to set-up (S) for this encounter.	Point E 47.315149°, -97.075449°	RPIC calls "holding at point e"	
	1d	UA exits (S) and proceeds towards SS once intruder begins exits its set-up turn.		Flight test director calls UA set up exit (USE).	
	1f	Altitudes are checked through radio calls.			
	2	Arrival time at the HEFP is within tolerance—Scenario Start (SS) is declared.	Difference between arrival times at HEFP is ≤ 6.5 s.	Flight test director calls SS.	
	3	Encounter Initiation (EI) is declared.	Occurs after SS and no later than approximate time of first alert or warning.	Flight test director calls EI.	

2

	4c	Time of Maneuver Initiation (MI) is recorded.	Data collector records the time of MI. If MI does not occur, this is noted.	RPIC calls "maneuvering"	
	5	Encounter End (EE) is declared.	Data collector records the time of encounter end (same as scenario end).	Flight test director declares EE.	
	6	Both aircraft proceed to set-up (S) for next encounter (if applicable).			

Manned Test Card

Flight Card #	A18-ND-MAN-DE-0_2-120	
Date/Time		
Objective		
Description	Manned aircraft and UAS encounters are conducted at the indicated cruise speeds. The manned aircraft starts at 1100 feet AGL and descends down to 800 feet AGL at 500 feet/min. A vertical offset of 400' used to provide safety margin.	
UAS Platform	Supervolo	
UAS Altitude	390 ft	
UAS Speed	40 knots	
Intruder	Piper Archer	
Intruder Altitude	1100 - 800 ft	

1

Intruder Speed	120 knots
Location	47.328505, -97.087696. Lovas Farmstead.
GCS	Mission Planner
DAA System ID	L3Harris GBDAA
DAA Sensors	Xtend ADS-B Receiver, C-Speed Radar, FAA NextGen (VAS)
Supporting Technology	NPUASTS trailers, visualization systems, additional ADS-B receivers, video cameras, DCAPS data recording
Intruder Pilot	
RPIC	
VOs	
MC	
FD	
COA/Waiver(s)	

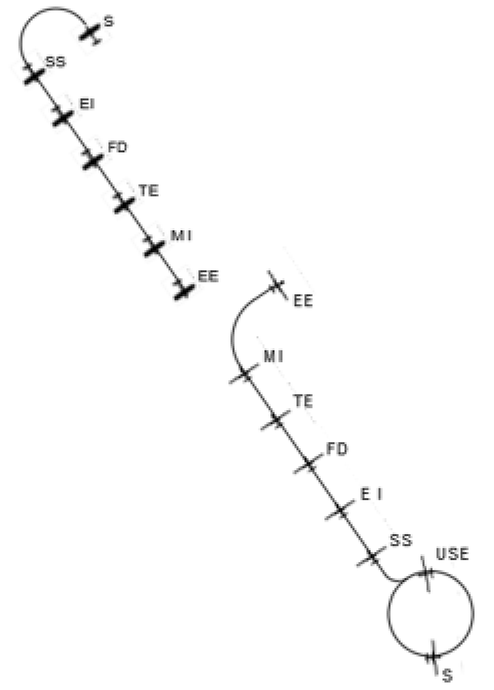

Condition # (objective)					
✓		Action	Remarks	Call	Time
	1b	Intruder executes turn at defined ground point ~17,160 ft (~3.25 mi) from HEFP during (S) at 1100 feet AGL.	This is driven by the DAA technology, the warning/alert system, and UA speed. 47.365509°, -97.126405°	Intruder calls "Holding NW"	
	1c	Intruder begins flying straight along its encounter path towards Scenario Start (SS).			
	1e	Intruder varies speed to ensure arrival at HEFP within tolerance.			
	1f	Altitudes are checked through radio calls.			
	2	Arrival time at the HEFP is within tolerance—Scenario Start (SS) is declared.	Difference between arrival times at HEFP is ≤ 6.5 s.	Flight test director calls SS.	
	2a	Intruder aircraft begins descending at 500 feet per minute down to 800 feet AGL.		Flight test director calls "begin descent"	

2

	3	Encounter Initiation (EI) is declared.	Occurs after SS and no later than approximate time of first alert or warning.	Flight test director calls EI.	
	4c	Time of Maneuver Initiation (MI) is recorded.	Data collector records the time of MI. If MI does not occur, this is noted.	RPIC calls “maneuvering”	
	5	Encounter End (EE) is declared.	Data collector records the time of encounter end (same as scenario end).	Flight test director declares EE.	
	6	Both aircraft proceed to set-up (S) for next encounter (if applicable).			